PLATINUM GROUP ELEMENT (PGE) GEOCHEMISTRY OF BRAZOS SECTIONS, TEXAS, U.S.A.

BRIAN GERTSCH AND GERTA KELLER
Department of Geosciences, Princeton University, Princeton NJ 08544, U.S.A.
e-mail: bgertsch@princeton.edu

THIERRY ADATTE
Institut de Géologie et Paléontologie, Université de Lausanne, Anthropole, CH-1015 Lausanne, Switzerland

AND

ZSOLT BERNER
Karlsruhe Institute of Technology, University, 76131 Karlsruhe, Germany

Abstract: Geochemical and sedimentological analyses of platinum group element (PGE) patterns across the Cretaceous–Tertiary (KT) transition of eight sections along the Brazos River, Texas, reveal possible sources and processes responsible for PGE enrichments. Of the five global characteristics defining the Cretaceous–Tertiary boundary (KTB) (mass extinction in planktic foraminifera, first appearance of Danian species, negative $\delta^{13}C$ excursion, Ir anomaly, thin (0.5 cm) red clay layer), the Ir anomaly and the red clay layer are not present at the KTB in the Brazos sections. Instead, PGEs and especially Ir show several minor enrichments within the sandstone complex, with the largest peak at the top or just above it. Possible mechanisms of PGE enrichments include low sedimentation rates or sediment starvation that concentrates Ir and other PGEs. Absence of Ir at the KTB is likely linked to dilution effects caused by high sedimentation rates, and other still unknown processes. The source of PGEs remains elusive, but it may be linked to an increased input of extraterrestrial dust during the late Maastrichtian, or reworked PGEs from the Chicxulub impact, which predates the KTB in these sections.

Key words: Iridium, PGE, KT boundary, Brazos River, Texas

INTRODUCTION

The mass extinction at the Cretaceous–Tertiary (KT) boundary (65 My) is well known for its possible causal link with an extraterrestrial impact based primarily on the presence of high iridium (Ir) concentrations (Alvarez et al., 1980). The discovery of the Chicxulub impact crater on Yucatán and the occurrence of impact-spherule ejecta at the base of a sandstone complex below the KT boundary in outcrops in Mexico and Texas seemed to confirm this hypothesis. Early studies interpreted this sandstone complex as impact-generated megatsunami deposit in order to temporally relate the impact spherules at the base of the sandstone complex with the Ir anomaly above it (e.g., Hildebrand et al., 1991; Hildebrand et al., 1995; Pope et al., 1991; Smit et al., 1992; Smit et al., 1996).

The megatsunami interpretation has been challenged based on the very same sections in northeastern Mexico and Texas. At these localities, multiple spherule depositional events and multiple horizons of trace fossils indicate that deposition of the sandstone complex occurred over an extended time period and is estimated to have been about 300,000 years prior to the KT boundary (Keller et al., 1997; Ekdale and Stinnesbeck, 1998; Keller et al., 2002; Keller et al., 2003a; Keller et al., 2007; Keller et al., 2009a). In northeastern Mexico the original Chicxulub spherule ejecta layer was discovered more than 4 m below the basal unconformity of the sandstone complex and its reworked spherules (Keller, 2008a; Keller, 2008b; Keller et al., 2009b). In Texas up to 80 cm of latest Maastrichtian claystone deposition separates the sandstone complex from the KT boundary, clearly marking the KT mass extinction and sandstone complex as two separate events. Moreover, a yellow clay layer consisting of altered impact glass spherules (cheto smectite) was discovered in claystone 45–60 cm below the basal unconformity of the sandstone complex (Keller et al., 2007; Keller et al., 2009a).

Thus, in both localities the oldest and presumably original impact-ejecta fallout was discovered in upper Maastrichtian sediments near the base of biozone CF1, which spans the last 300,000 years of the Maastrichtian and indicates that the Chicxulub impact predates the KT mass extinction. These results from Mexico and Texas were also confirmed by the Yaxcopoil-1 well, drilled within the Chicxulub crater where the suevite breccia is separated from the KT boundary by 50 cm of laminated limestone with zone CF1 foraminifera deposited in C29r over a long time period as indicated by five thin glauconite layers (Keller et al., 2004a; Keller et al., 2004b).

Proponents of the impact tsunami contested these results largely on the basis that slumps, gravity flows, and large-scale earthquake disturbances can account for the age discrepancies (Bourgeois et al., 1988; Smit et al., 2004; Alegret et al., 2005; Schulte et al., 2006; Schulte et al., 2008; Kring, 2007). However, no large-scale or even significant disturbances are observed or documented in northeastern Mexico or Texas. In the crater core Yaxcopoil-1, high-energy deposition marks the top of the suevite breccia well prior to deposition of the 50-cm-thick limestone layer (Keller et al., 2004a; Keller et al., 2004b). Moreover, large-scale disturbances in Yaxcopoil-1 could not account for the limestone deposition with trace fossils, five glauconite layers, zone CF1 foraminiferal assemblages, C29r paleomagnetic signals, and typical late Maastrichtian $\delta^{13}C$ signals followed by the characteristic negative $\delta^{13}C$ shift at the KT boundary.

A major reason for the KT boundary controversy is the belief that the Ir anomaly and impact spherules have the same origin and therefore must have been deposited at the same time (see comment by Schulte et al., 2008, and reply by Keller et al., 2008a). Based on this premise, all

The End-Cretaceous Mass Extinction and the Chicxulub Impact in Texas
SEPM Special Publication No. 100, Copyright © 2011
SEPM (Society for Sedimentary Geology), Print ISBN 978-1-56576-308-1, CD/DVD ISBN 978-1-56576-309-8, p. 227–249.

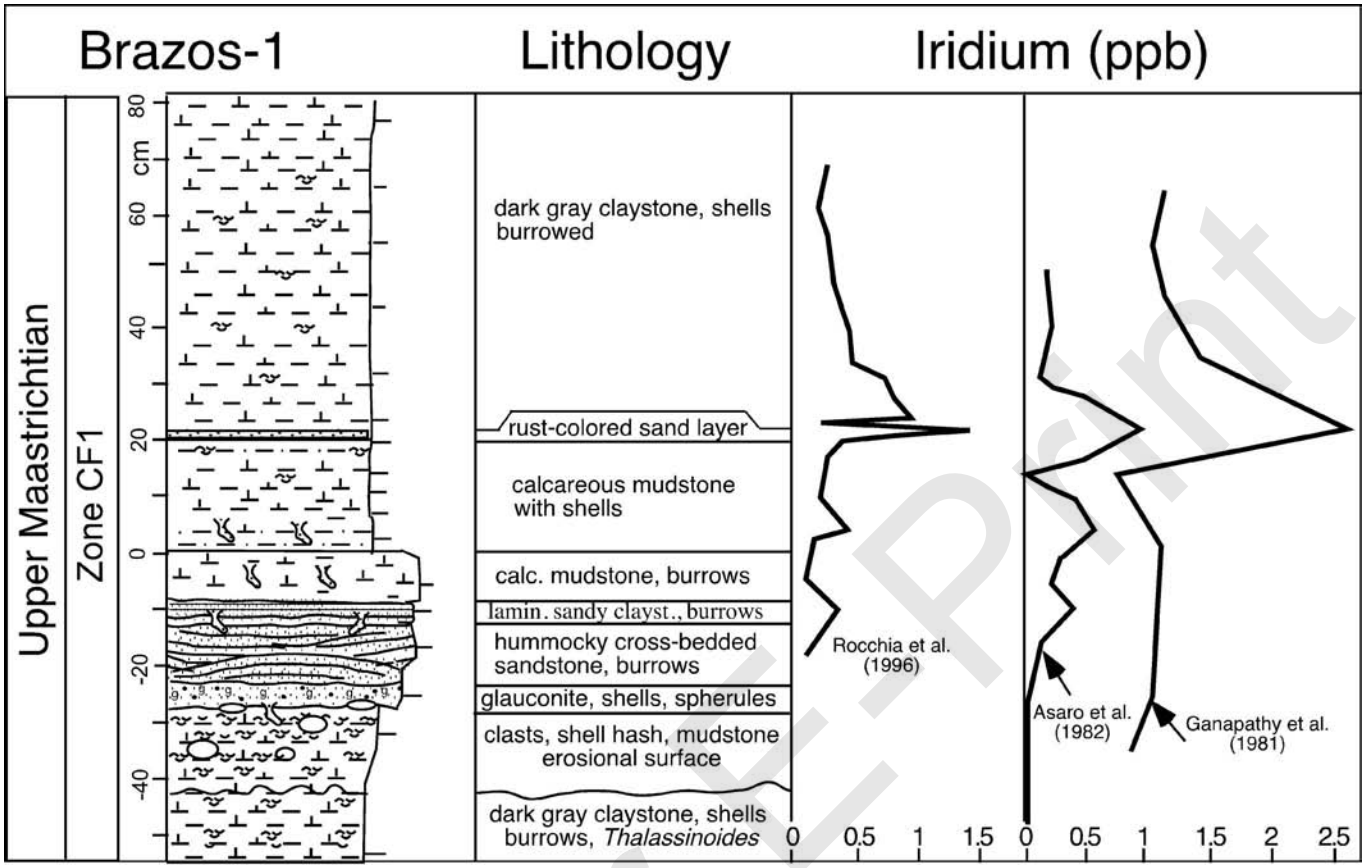

FIGURE 1.—First Ir results by Ganapathy et al. (1981), Asaro et al. (1982), and Rocchia et al. (1996) at Brazos-1 with a significant peak in Ir of variable intensity in a rust-colored sand layer.

contrary data must be explained as artifacts of the sedimentary record, which becomes difficult when the sum total is overwhelmingly against a coeval common origin for impact spherules and an iridium anomaly from the Chicxulub impact. In the late 1980s the sandstone complex was interpreted as impact-generated and therefore marking the KTB (Bourgeois et al., 1988). Others interpreted the Ir anomaly above the sandstone complex as better marker for the KTB and justified this placement on the basis of changes in nannofossil abundances (Jiang and Gartner, 1986) and a rare isolated occurrence of early Danian planktic foraminifera (Keller, 1989). Both KTB placements were wrong and could not be confirmed in subsequent studies (Keller et al., 2007; Keller et al., 2009a; Tantawy, this volume).

This controversy is thus largely based on poor knowledge of extraterrestrial signals and their relationships, including Ir, impact spherules, and shocked quartz. This is demonstrated in Central and North America where the Ir enrichment and spherule-rich layers are never at the same stratigraphic horizon and impact spherules are never observed at the KT boundary where this boundary transition is most complete (review in Keller, 2008).

The Brazos sections, with their multiple Ir enrichments and impact-spherule layers are an excellent example of this puzzling pattern. They contain multiple impact-spherule layers in a sandstone complex, an altered impact-glass layer (cheto smectite) in mudstone below, up to three distinct Ir enrichments, but none coinciding with impact spherules, and the KT mass extinction up to 80 cm above the sandstone complex (Keller et al., 2007; Keller et al., 2009a).

The iridium record of the Brazos sections has presented a major challenge from the very beginning. The first investigations by Ganapathy et al. (1981) and Asaro et al. (1982), followed by Rocchia et al. (1996), revealed the major anomaly (~ 1.5 ppb) with maximum enrichment in a brown clay layer 3–4 mm thick and overlying a rusty sand layer 1 cm thick (Fig. 1). In the sandstone complex below, two minor (0.3 and 0.5 ppb) Ir concentrations were recorded. In the 1985 Snowbird meeting in Utah the placement of the KT boundary at the base of the sandstone complex conflicted with the Ir anomaly in the sediments above, which led Frank Asaro to call the Ir distribution uninterpretable "rubbish". Since that time we have analyzed patterns of five PGEs (Ir, Pd, Pt, Rh, Ru) in eight sections along the Brazos River and uncovered a consistent pattern of multiple enrichments none of which are associated with the KT boundary. Because it necessitates a different method of preparation and specific laboratory facilities, the last PGE, Os, was not measured. For the purpose of this chapter, the term "PGE" therefore refers only to Ir, Pd, Pt, Rh and Ru.

Main Objectives and Testing Hypotheses

The main objectives of this study are to evaluate the Ir, Pd, Pt, Rh, and Ru records of the Brazos sections, determine their relationship to the Chicxulub impact and the KT mass extinction, and determine their possible origin(s). The little studied and puzzling Ir record of the Brazos sections offers a great opportunity to study the geochemical behavior of PGEs in response to the terminal Cretaceous events in a shallow nearshore environment. We hope to gain insights into the following questions: Are Ir and other PGE anomalies correlatable?

What is the nature and origin of the Ir anomalies? Are enrichments due to extraterrestrial or volcanic sources? Can they be mobilized and/or concentrated during times of low sedimentation or nondeposition? What is the role of redox conditions in Ir enrichments? Why are maximum Ir enrichments in most Brazos sections in the hummocky cross-bedded sandstone interval or in the overlying laminated sandstone of the sandstone complex? Why are major geochemical (Ir, Pd, Pt, Rh, Ru) and lithological (red layer, clay) markers of the KT boundary absent at Brazos? Careful geochemical and lithological studies of Brazos sections contribute at least partial answers to these questions and provide directions for further research.

The Brazos KT transition is unique in that deposition occurred in a very shallow (< 30 m) nearshore environment with high terrigenous influx and sea-level fluctuations that resulted in alternating high and low sedimentation rates, as well as erosion and/or nondeposition (Gale, 2006; Keller et al., 2007). These variable sedimentation rates, and possibly local redox conditions, may have been the predominant factors responsible for concentrating the studied PGEs at specific levels and diluting them in others (e.g., absence of distinctive KT red clay layer). To test these hypotheses we chose several complete sections in the Brazos area spanning the late Maastrichtian–early Danian interval and concentrated on sedimentology and PGE distribution.

PGE DISTRIBUTION ACROSS THE KT TRANSITION: BACKGROUND

An Ir anomaly is a major supporting characteristic for an extraterrestrial impact and is commonly found in a thin red oxidized clay layer at the KT boundary worldwide (Alvarez et al., 1980, Graup and Spettel, 1989; Bhandary et al., 1994; Stueben et al., 2005). Iridium is one of the platinum-group elements (PGEs) together with Pt, Pd, Rh, and Ru (Sawlowicz, 1993), all of which behave as siderophile and chalcophile elements, except for Ir, which has a lithophile behavior (Campell et al., 1983; Amosse and Alibert, 1993; Peach et al., 1994; Kramar et al., 2001). PGEs are generally present in extremely low concentrations on Earth (Wedepohl, 1995) but can form anomalous concentrations in sediments due to several sources (e.g., extraterrestrial, volcanic, hydrothermal), and processes (e.g., continental weathering, eustatic fluctuations, biological processes, precipitation from seawater, and redox-controlled enrichment; Sawlowicz, 1993; Kramar et al., 2001).

Extraterrestrial materials are a significant source of PGEs due to their high PGE contents (Table 1). For example, iron meteorites contain 24,000–30,000 ng/g Ir (Wasson et al., 1989), and Ir concentrations in chondritic meteorites range from 338 to 810 ng/g (Kalleymeyn et al., 1989). Volcanism has been suggested as a major source of PGE enrichment, especially iridium (Zoller et al., 1983; Officer et al., 1987; Hallam, 1987). PGE distribution during magmatic evolution is mainly linked to the sulfur cycle (Keays, 1995; Kramar et al., 2001) and compared with Ir leads to chondrite-normalized Ru, Rh, Pt, and Pd enrichments (Barnes et al., 1985; Keays, 1995). Hydrothermal enrichments in PGEs are also postulated, but the behavior of each element varies individually depending on temperature and fluid composition (McCallum et al., 1976; Patkunc and Ghandi, 1989; Crocket, 2000).

PGE anomalies can also originate from continental weathering of ore deposits, mafic rocks, and ultramafic rocks (Sawlowicz, 1993), but they often leave a contradictory signal (McCallum et al., 1976). At the seawater–sediment interface, dissolved PGEs are removed from the water column by precipitation and co-precipitation with (bacterial) iron

TABLE 1.—PGE abundances measured in chondrites, bulk continental crust, Deccan basalt, sediments (anoxic, euxinic, Mn-nodules), seawater and various KT layers are compared to identify the potential origin of PGEs at the KT boundary.

	Ir (ppb)	Pd (ppb)	Pt (ppb)	Rh (ppb)	Ru (ppb)	
PGE abundances						
Chondrites	481	560	990	134	712	Anders and Grevesse, 1989
Bulk continental crust	0.037	1.5	1.5	0.4	0.6	Bertine et al., 1993; Rudnick and Gao, 2003
Deccan basalt	0.036	11.9	4.3	0.08–0.58	0.13–0.72	Crocket and Paul, 2004; Crocket and Paul, 2008
Pelagic sediments (carbonate poor)	0.3–0.4	3.2–3.5	3–3.8	0.6	0.15–1	Crocket and Huo, 1979; Bekov et al., 1984; Colodner, 1991; Bertine et al., 1993
Anoxic sediments	<1	28	30	<1	<1	Li and Gao, 2000
Euxinic sediments	4 ± 0.8	396 ± 58	342 ± 52.7	15.8 ± 2.5	7.3 ± 2.8	Lehman et al., 2007
Manganese nodules	1.1–2.6	0.9	100–265	14	1.6–14.5	Bekov et al., 2004; Goldberg et al., 1986; Colodner, 1991; Bertine et al., 1993
Seawater	0.001	0.02–0.06	0.1–0.2	0.05–0.1	0.001–0.002	Bekov et al., 1984; Bertine et al., 1993
K/T layers						
Meghalaya K/T, India	12	73.86	86.48	93.44	108.24	Gertsch et al., in prep
El Kef K/T, Tunisia	17	n/d	n/d	n/d	n/d	Rocchia et al., 1996
Mishor Rotem K/T, Israel	3.2	4	2.2	0.26	1.5	Adatte et al., 2005
Gubbio K/T, Italy	7	n/d	n/d	n/d	n/d	Rocchia et al., 1990
Koshak K/T, Kazahkstan	4	n/d	n/d	n/d	n/d	Pardo et al., 1999
Stevns Klint K/T, Denmark	14.88–54	55–105	201–210	n/d	n/d	Schmitz, 1988; Tredoux et al., 1989
Brazos (Maastrichtian), Texas, USA	0.1–1.4	0.2–48	1.0–22	0.1–0.4	0.3–1.2	This study

oxides and sulfides, as well as by scavenging in ferromanganese phases (Playford et al., 1984; Dyer et al., 1989; Wallace et al, 1990; Colodner et al., 1992; Anbar et al., 1996). In marine sediments the dissolution effect, diagenetic postdepositional remobilization, and redox-controlled precipitation lead to secondary enrichments accompanied by other trace elements (Ekdale and Bromley, 1984; Colodner, 1991; Colodner et al., 1992; Sawlowicz, 1993; Evans et al., 1994; Piestrynski and Sawlowicz, 1999). Small Ir anomalies also correlate with marine flooding surfaces (MSFs) suggesting that Ir is concentrated in marine sediments during periods of terrigenous-sediment starvation (Donovan et al., 1988; Stinnesbeck et al., 1999).

Melt-rock spherules are first-order evidence for extraterrestrial impacts. Chicxulub impact spherules are concentrated in spherule-rich layers in upper Maastrichtian and lower Danian outcrops around the Gulf of Mexico, including northern Mexico (Keller et al., 1994, Stinnesbeck et al., 2001; Schulte et al., 2003; Keller et al., 2003a; Keller et al., 2009b), Texas (Bourgeois et al., 1988; Gale, 2006; Schulte et al., 2006; Keller at al, 2007), Belize and Guatemala (Stinnesbeck et al., 1997; Keller et al., 2003b), Cuba (Alegret et al., 2005), and Haiti (Jehanno et al., 1992; Koeberl, 1992; Leroux et al., 1995; Stinnesbeck et al., 1999; Keller et al., 2001). The best outcrops are in northeastern Mexico and Texas, where up to four spherule-rich layers are present, including the original fallout and subsequently reworked spherule layers interbedded in upper Maastrichtian sediments. But no spherules are observed at the KT boundary, which is defined by micropaleontological and geochemical proxies (the mass extinction in planktic foraminifera, the first appearance of Danian species, a 2–3‰ $\delta^{13}C$ negative shift, and an Ir anomaly (Keller et al., 1995; Keller et al., 2008a). Spherules have been observed at the KT boundary only in condensed or incomplete deep-sea sections (Norris et al., 1999; MacLeod et al., 2006; Keller, 2008). The absence of impact spherules in expanded sections illustrates the problems encountered in equating the age of the Chicxulub impact with the KT Ir anomaly.

PGE GEOCHEMISTRY

Iridium

Iridium (Ir) is an important PGE due to the high quantities present in chondrites and very low concentrations in the bulk continental crust, basalts, and different types of sediments (Table 1). Anoxic sediments are not major sinks for Ir (Anbar et al., 1996), but euxinic sediments are slightly more enriched (Lehmann et al., 2007). Due to these large differences, Ir has been widely used as a proxy for extraterrestrial impacts.

In pelagic sediments Ir is enriched mainly by accommodation in authigenic ferromanganese oxyhydroxides and rarely by extraterrestrial input (Barker and Anders, 1968; Goldberg et al., 1986; Kyte and Wasson, 1986). Because of its strong enrichment in manganese nodules (Table 1), Ir appears to be involved in the manganese cycle in marine sediments. In pelagic sediments, Ir seems to be incorporated into hydrogenous Fe-Mn oxyhydroxide minerals and is therefore remobilized when these phases are reduced (Colodner, 1991; Colodner et al., 1992). These results are in accordance with Ir seawater chemistry (Anbar et al., 1996) and demonstrate that Ir is highly sensitive to postdepositional mobility caused by redox fluctuations. Colodner (1991) estimated that if Ir lost from halos (i.e., a zone of reduction below a lithostratigraphic boundary) in recent sediments during early or late diagenesis were trapped in a layer 1 cm thick, the resulting peak would reach concentrations from 0.8 to 1.6 ppb.

Platinum

Platinum (Pt) is the main PGE present in chondrites and bulk continental crust (Table 1). In Deccan volcanic basalts Pt is the second most abundant PGE, with concentrations similar to those in bulk continental crust (Table 1). In seawater, Pt shows the highest concentrations among all PGEs (Bertine et al., 1993).

Pt is a siderophile and chalcophile element (Colodner, 1991) and belongs to noble metals due to its high resistance to oxidation (Westland, 1981). Pt is very abundant in manganese nodules (Table 1) and is enriched in pelagic sediments due to accommodation of authigenic ferromanganese oxyhydroxides, and to a lesser extent, contributions from cosmic dust (Barker and Anders, 1968; Goldberg et al., 1986; Kyte and Wasson, 1986). More recent studies show that Pt occurs in association with both organic-rich sediments deposited under anoxic and euxinic conditions, as well as with hydrogenous ferromanganese oxides in sediments (Colodner, 1991; Colodner et al., 1992; Li and Gao, 2000; Lehmann et al., 2007). Therefore, Pt is highly sensitive to redox fluctuations and is subject to postdepositional remobilization within the sedimentary column (Colodner, 1991; Colodner et al., 1992).

Palladium

Palladium (Pd) shows average contents in chondrite, but it is the most abundant PGE in the bulk continental crust and basalts (Table 1). In seawater, Pd is relatively high compared to other PGEs (Bertine et al., 1993). Pd shows very low concentrations in manganese nodules, in contrast to most PGEs (Table 1; Goldberg, 1987). Pd is the most abundant in organic-rich sediments deposited under euxinic conditions (Table 1). In pelagic sediments, Pd originates mainly from a terrigenous source (Crocket et al., 1973; Crocket and Hu, 1979) and is generally considered as the most mobile PGE due to its very high solubility (Cousins and Vermaak, 1976; Westland, 1981; Evans and Chai, 1997).

Rhodium

Rhodium (Rh) is the least abundant PGE in chondrite and sediments (Table 1), but it has the second highest concentration in seawater (Bertine et al., 1993). In pelagic sediments, Rh concentrations are fairly constant, except in rare samples with high contents in Bi, Co, Mn, and other PGEs (Goldberg et al., 1986; Bertine et al., 1996). High Rh concentrations are observed in organic-rich sediments deposited under euxinic conditions (Table 1; Lehmann et al., 2007). Rh shows a low mobility during weathering processes (Cousins and Vermaak, 1976; Westland, 1981).

Ruthenium

Ruthenium (Ru) is the second most abundant PGE in chondrites and shows low concentrations in the bulk continental crust and Deccan basalts (Table 1). In seawater, Ru is rare (Bertine et al., 1993). In sediment, Ru shows highest concentrations in organic-rich sediments deposited under euxinic conditions (Lehmann et al., 2007).

METHODS

All sections presented in this paper were examined during various fieldtrips to Texas between 2005 and 2007. Each section was described, measured, and sampled at closely spaced intervals of 5 to 10 cm. In critical intervals (e.g., the sandstone complex), sample spacing was closer.

The determination of the PGE concentrations was carried out at Karlsruhe University using pre-concentration with Ni-fire assay coupled with quantification by isotope dilution (ID) and high-resolution ICP-MS (Axiom, VG). About 10 g of the well-homogenized sample material was dried at 105°C and ignited at 450° and 950°C until constant weight. After cooling, the sample was mixed with 15 g of

Na_2CO_3, 50 g of sodium tetraborate, 5 g of nickel powder, 4 g of sulfur, and 12 g of analytically pure quartz sand. By fusing at 1140°C for 1 h, the melt segregates to a silicate and Ni-sulfide phase where the "Ni-button" or "regulus" collects the PGEs. After cooling, the regulus was crushed and its bulk (NiS) dissolved at 90°C in HCl_{conc}. After filtration through PTFE-membrane filter, the residue was dissolved in a mixture of H_2O_2 and HCl_{conc}. By heating slowly, the solution was subsequently dried and taken up with 1% HNO_3 in 10 ml flasks. All chemicals used in the digestion of the PGEs were of suprapure grade.

PGE concentrations in the solution were measured by high-resolution ICP-MS (Table 2, 3). At the beginning of each analytical batch, in a first step, the actual PGE concentrations in the spike solution used was determined by interchanging the role of spike and sample ("inverse isotope dilution technique"). Reported values for Ru, Pd, and Pt are the mean of concentrations calculated on basis of two or three different ratios ($^{99}Ru/^{101}Ru$, $^{99}Ru/^{102}Ru$; $^{105}Pd/^{108}Pd$, $^{105}Pd/^{104}Pd$; $^{194}Pt/^{198}Pt$, $^{195}Pt/^{198}Pt$, $^{196}Pt/^{198}Pt$, respectively). Despite the high accuracy and reliability of the isotope dilution technique, some variance and problems may occur, notably if the isotopes involved are affected by overlaps with molecule clusters generated in the plasma. Isobaric interferences on the considered PGE isotopes were corrected taking into account the abundance of an undisturbed isotope (e.g., ^{104}Ru on ^{104}Pd, based on the abundance of ^{101}Ru, and ^{102}Pd on ^{102}Ru, based on ^{104}Pd).

The content in the monobaric Rh was determined by applying a correction factor for recovery as resulted from the ratio between the concentrations of Pt and Ir quantified with and without isotope dilution. Recoveries for Rh were found to be generally between 70 and 80%. Because available certified PGE standards (e.g., WPR-1/CANMET; SARM7) have much higher concentrations than in the samples, accuracy was checked by analyzing an in-house laboratory standard (ODP basalt), characterized on basis of analyses carried out over many years. Deviation of the mean value of the ODP standard processed together with the samples from its multi-annual average was found to be +16% for Ru, +6% for Rh, −4% for Pd, +1% for Ir, and −11% for Pt. Detection limits, assessed on basis of the threefold standard deviation of the procedural blanks, was found to be 0.5, 0.06, 0.9, 0.2, and 0.4 ng/kg for Ru, Rh, Pd, Ir, and Pt, respectively.

PLATINUM-GROUP ELEMENTS (PGEs): RESULTS

The Brazos sections used for PGE analysis are located along a NE–SW transect west of the Brazos River (Fig. 2). The outcrops and wells are from three geographically separated localities that show significant lithological changes over short distances.

Core Mullinax-1 (Mull-1)

The Mull-1 core was drilled on a meadow 370 m south of the Highway 413 Bridge across the Brazos River, Falls County, Texas (GPS Location 31° 07′ 53.00″ N, 96° 49′ 30.14″ W; Fig. 2). The studied interval for PGEs spans from 7 m to 8.8 m depth and encompasses the main part of the sandstone complex, the overlying uppermost Maastrichtian claystone, the KT boundary, and the lower Danian (P0 and P1a) (Fig. 3; for age and lithological description see Keller et al., this volume; Adatte et al., this volume).

The sandstone complex is subdivided into six units (Keller et al., 2007) and usually records low concentrations in the upper part of unit 2 of the spherule-rich coarse sandstone (SCS), a calcareous upward-fining sandstone, and in the overlying bioturbated hummocky cross-bedded sandstone (HCS) of unit 4 (Ir, < 0.1 ppb; Pd, 1 ppb; Pt, 2 ppb; Rh, 0.1 ppb; Ru, 0.4 ppb; Fig. 3). However, Pd peaks within unit 4 (22 ppb), whereas Ir, Pt, Rh, and Ru concentrations show maxima at the base of unit 5 in a bioturbated contact, with 1.5 ppb, 5 ppb, 0.4 ppb, and 2.1 ppb, respectively. Unit 6 consists of a fining-upward calcareous

TABLE 2.—PGE concentrations measured by high resolution ICP-MS at Cottonmouth Water Fall, CM4, Darting Minnow Creek sections, and Mullinax-1 core.

	Ru [ppb]	Rh [ppb]	Pd [ppb]	Ir [ppb]	Pt [ppb]
CM Water Fall section					
CMW-7	0.26	0.04	0.71	-	1.04
CMW-8a	0.64	0.05	0.88	-	1.72
CMW-8b	0.18	0.29	2.61	-	1.47
CMWF-13	-	-	-	0.24	-
CMWF-14–1	-	-	-	<0.2	-
CMWF-14–2	-	-	-	<0.2	-
CMWF-14-a	-	-	-	<0.2	-
CMWF-15	-	-	-	<0.2	-
CMWF-22a	-	-	-	<0.2	-
CMWF-23	-	-	-	<0.2	-
CM4 Section					
CM4–5	0.85	0.11	1.79	0.69	1.11
CM4–7	0.92	0.12	1.05	0.20	6.07
CM 4–9	0.77	0.09	0.79	0.52	4.68
CM 4–10	0.58	0.07	0.92	0.32	10.35
CM 4–11	0.53	0.09	0.56	0.32	3.20
CM 4–12	-	-	-	0.27	-
CM 4–14	-	-	-	0.24	-
CM 4-Kr	-	-	-	<0.2	-
CM 4-Py	-	-	-	0.26	-
Minow Creek Section					
DMC-1	0.35	0.05	1.49	<0.2	1.85
DMC-2	0.41	0.03	0.06	<0.2	0.35
DMC-3	0.34	0.02	0.45	<0.2	2.09
DMC-5	0.58	0.07	1.06	<0.2	1.35
DMC-Konkr.	1.93	0.02	1.14	0.66	8.57
Mullinax 1 Core					
Mull-15	0.30	0.10	1.91	0.20	6.26
Mull-16	0.40	0.12	<1	0.20	48.32
Mull-18	0.36	0.19	1.25	0.23	6.67
Mull-19	0.44	0.10	<1	0.13	8.12
Mull-20	0.41	0.12	<1	0.17	3.04
Mull-21	0.43	0.31	<1	0.15	10.53
Mull-22	0.33	0.12	<1	0.14	3.74
Mull-24	0.30	0.10	<1	<0.1	2.04
Mull-25	0.80	0.10	<1	0.21	3.54
Mull-26	0.34	0.18	1.49	0.17	1.70
Mull-28	0.30	0.11	1.44	0.14	2.50
Mull-30	0.31	0.13	<1	0.25	1.24
Mull-31	0.49	0.10	1.18	0.37	2.54
Mull-34	0.75	0.17	1.66	0.63	2.93
Mull-38	1.45	0.41	1.25	0.83	2.54
Mull-42	0.64	0.33	48.59	0.67	3.00
Mull-45	1.00	0.36	1.90	0.74	5.48
Mull-47	2.06	0.38	2.18	1.43	4.30
Mull-50	0.54	0.10	22.65	0.12	1.70
Mull-58	0.38	0.10	0.87	<0.1	1.59

TABLE 3.—PGE concentrations measured by high resolution ICP-MS at CMA, CMB and River Bed sections.

	Ru [ppb]	Rh [ppb]	Pd [ppb]	Ir [ppb]
CMB section				
CMB 16	0.30	0.08	1.01	0.13
CMB 15	0.62	0.10	1.49	0.04
CMB 13	0.17	0.08	0.70	0.04
CMB 12	0.21	0.10	3.29	0.14
CMB 11	0.66	0.18	1.97	0.14
CMB 10	0.30	0.12	0.72	0.13
CMB 09	0.28	0.12	0.69	0.12
CMB 08	0.42	0.14	0.38	0.15
CMB 07	1.09	0.27	1.44	0.54
CMB 06	0.35	0.05	1.26	0.26
CMB 05	0.47	0.29	1.37	0.33
CMB 04	0.79	0.16	0.93	0.51
CMB 03	0.39	0.12	0.91	0.44
CMB 02	0.23	0.15	0.56	0.21
CMB 01	0.80	0.18	1.36	0.54
CMA sections				
CMA 21	0.47	0.14	0.46	0.42
CMA 20	0.22	0.05	0.70	0.10
CMA 18	0.30	0.10	0.70	0.16
CMA 16	0.96	0.14	0.52	0.42
CMA 15	0.30	0.10	1.54	0.10
CMA 13	0.30	0.08	0.70	0.10
CMA 12	0.39	0.10	0.64	0.15
CMA 11	0.30	0.07	0.96	0.10
CMA 10	0.30	0.10	0.70	0.10
CMA 07	0.30	0.06	0.70	0.10
CMA 05	0.30	0.07	0.64	0.10
CMA 04	0.56	0.14	0.98	0.23
CMA 03	0.18	0.09	0.57	0.13
CMA 02	0.30	0.08	0.40	0.10
CMA 01	0.30	0.06	0.70	0.10
CMA 00	0.30	0.09	0.68	0.10
CMA (−1)	0.30	0.10	0.50	0.10
CMA (−2)	0.30	0.07	0.70	0.10
CMA (−3)	0.18	0.10	0.70	0.10
River Bed Section				
BR1–2				<0,2
BR1–4				<0,2
BR1–6				<0,2
BR1–9				<0,2
BR1–10				1.13
BR1–11				<0,2
BR1–12				<0,2
BR1–13				<0,2
BR1–14				0.23
BR1–16				<0,2
BR1–18				<0,2

claystone recording a peak in Ir of 0.8 ppb followed by a gradual decrease to 0.6 ppb. Pt and Rh decrease to 3 ppb and 0.3 ppb, respectively, with a slight increase near the top, whereas Pd and Ru values remain stable (< 2 ppb and ~ 0.65 ppb), except for a single peak at 48 ppb and 1.4 ppb, respectively. The maximum in Pd is observed close to the base of unit 6 near a lithological change. Above the sandstone complex, Ir and Rh values decrease to 0.2 and 0.1 ppb in the lower part of the claystones and then remain below 0.2 ppb, Ru gradually decreases to 0.3 ppb, but with a single peak at 0.8 ppb at the end of the studied interval, whereas Pd and Pt concentrations remain steady at 0.1 and 0.2 ppb, respectively. There is no change in PGE concentrations at the KT boundary.

Brazos River-1

The Brazos River-1 section consists of exposures located in the riverbed that can be accessed at times of low water flow and covers mainly the sandstone complex (Fig. 2, after Munsel et al., this volume). The lithological sequence of the sandstone complex is considerably different from that in the nearby core Mull-1 (Fig. 4, see Adatte et al., this volume, for detailed description). The principal differences are in the number of repeated layers of shell hash, of sandstone rich in glauconite and shells, and of spherules-rich sandstone.

For Brazos River-1 Ir was the only PGE measured and shows usually low background concentrations (0.1 ppb) across the sandstone complex (Munsel et al., this volume). Two intervals record a single peak, respectively at 1.2 ppb in a clay layer with spherules and glauconite (#10, Fig. 4), and at 0.22 ppb in a sandstone layer with spherules (#14, Fig. 4).

The Brazos-2 and Brazos-3 Sections

Brazos-2 and Brazos-3 are two small outcrops about 10 m apart and located at the confluence of Cottonmouth Creek and the Brazos River (Fig. 2). Both sections show similar lithologies and are therefore shown as one litholog, which consists of the sandstone complex followed by silty–sandy shale, a limestone-concretion layer, calcareous claystone, and a second limestone-concretion layer (Fig. 5, Adatte et al., this volume).

In these sections Ir is the only quantified PGE element, and its concentrations remain at or below 0.1 ppb for the entire sequence at Brazos-2, except for one single value at 0.2 ppb (35 cm, zone P0) in bioturbated sandy shale. Higher overall Ir concentrations (0.1–0.2 ppb) are observed at Brazos-3, along with peak values of 0.7 ppb immediately above the sandstone bed and another increase to 0.5 ppb at the base of zone P0 that marks the KT boundary in bioturbated sandy shale (Keller et al., this volume). These two peaks are separated by very low values (0.1 ppb).

CM4 Section

The CM4 section is located along the Cottonmouth River about 250 m from the Cottonmouth Creek waterfall towards the Brazos River (Fig. 2). This section starts at the top of the sandstone complex and continues with claystone and gray glauconitic siltstone (Fig. 6, Adatte et al., this volume).

Ir distributions in the CM4 section are very similar to Brazos-3, with maximum Ir concentrations (0.7 ppb) in claystone immediately above the sandstone complex and a second peak (0.5 ppb) 20 cm above, followed by gradually decreasing concentrations to 0.2 ppb by KT boundary time (Fig. 6). Rh and Ru concentrations remain low and stable (0.1 and 0.9 ppb), whereas Pd values decrease from 1.8 to 0.6 ppb. Pt data increase rapidly from 1.1 to 10.3 ppb at the KT boundary and then drop sharply to 3.2 ppb.

Cottonmouth Creek CMAW-CMB Sections

The CMA-CMB section is a composite of three outcrops located near the Cottonmouth Creek waterfall (Fig. 2). The CMA and CMW outcrops are only 10 m apart, with the latter section sampled directly at

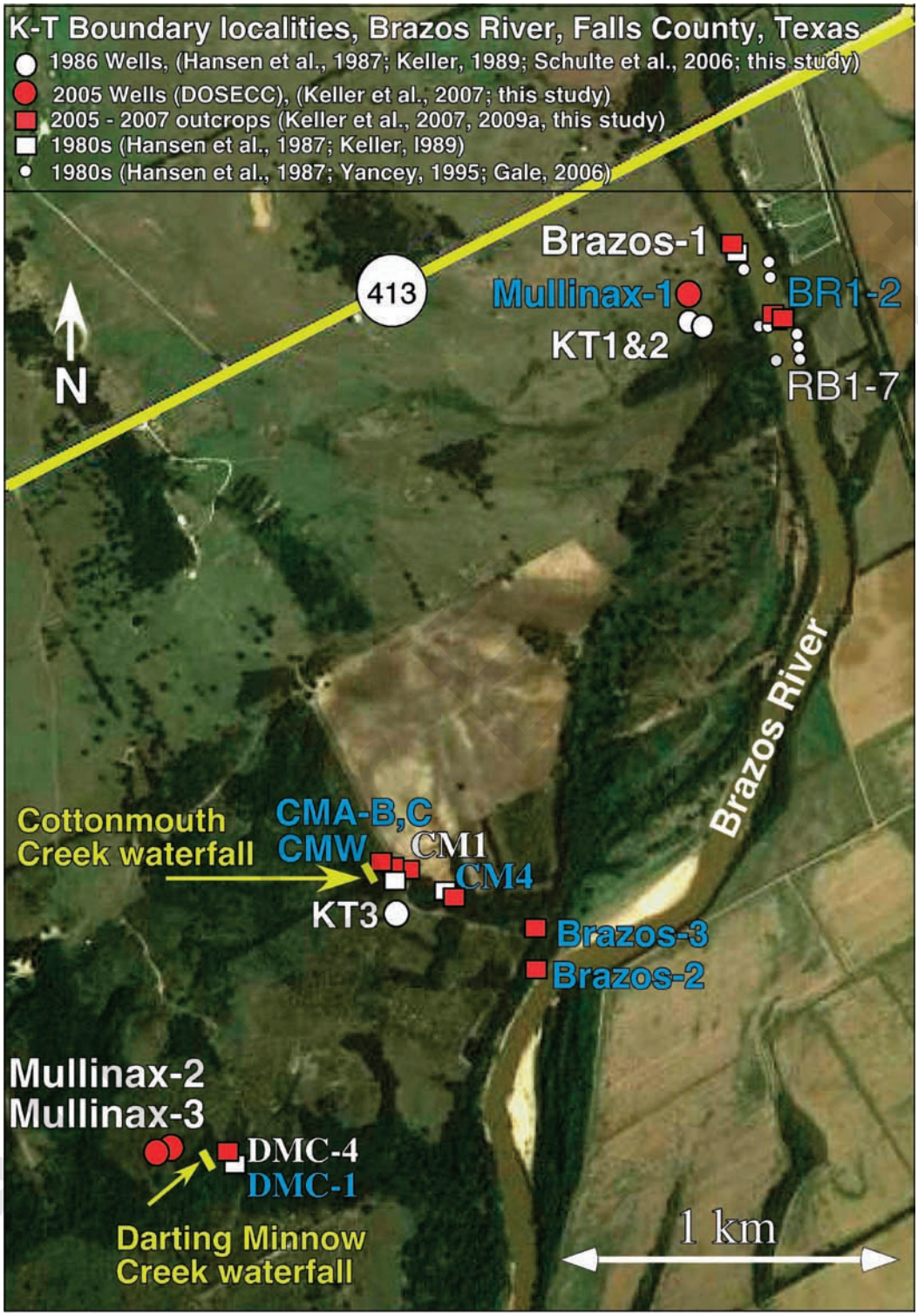

FIGURE 2.—Satellite map of the Brazos area with all the sampled sections and cores from various fieldtrips from 1986 to 2007. Sections and cores are grouped in three areas: (1) along the Brazos River, (2) near Cottonmouth Waterfall, and (3) near Darting Minnow waterfall.

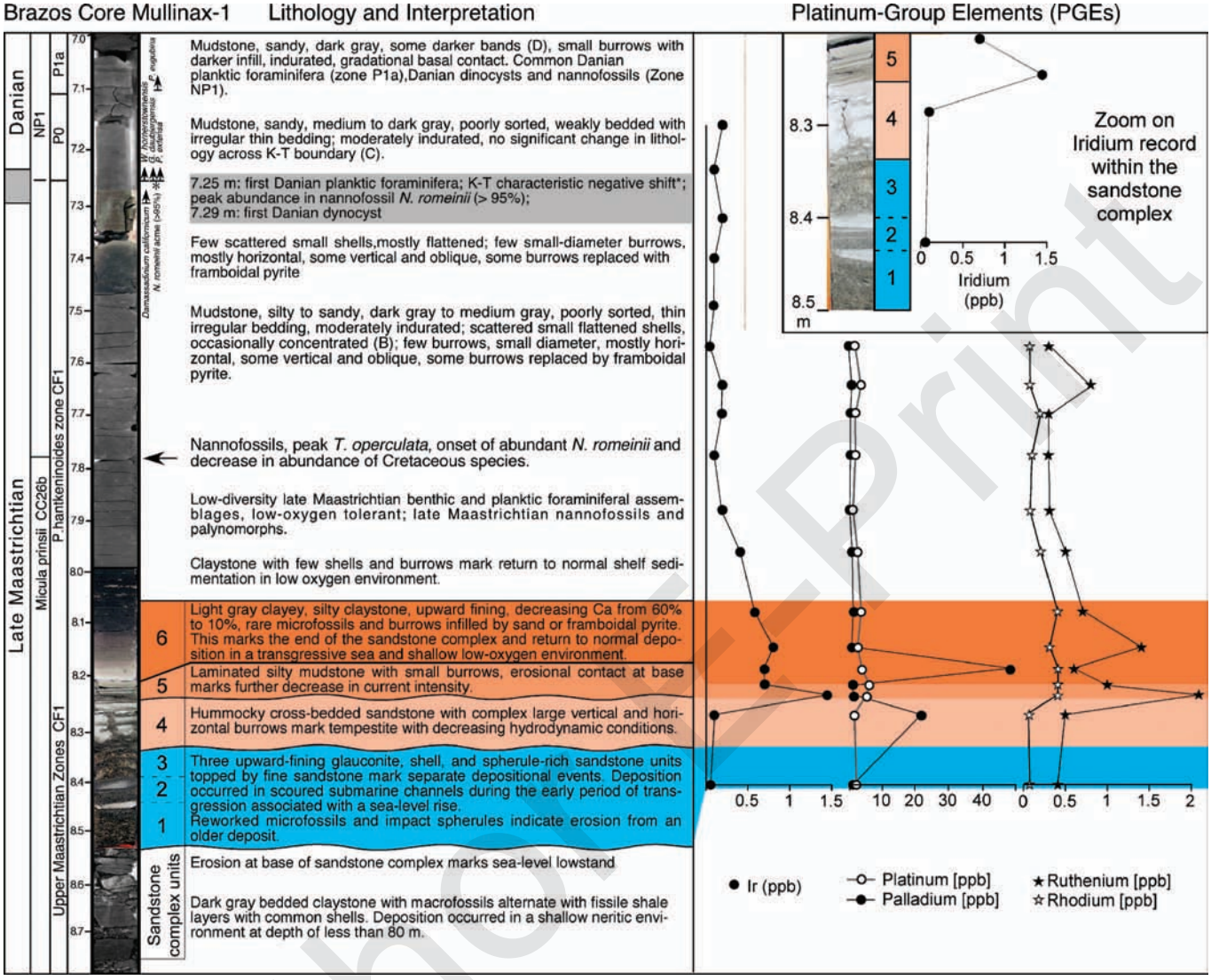

FIGURE 3.—Lithological description and Platinum Group Elements (PGEs) record of the late Maastrichtian–early Danian interval for the core Mullinax-1. Several PGE peaks occur in the sandstone complex, but usually not at the same level. Ir peaks at 1.4 ppb in a thin laminated silty mudstone.

the waterfall. Both sections span the same intervals (though CMA is now covered by a landslide) of upper Maastrichtian sediments up to 25 cm above the sandstone complex. The CMB outcrop spans from the sandstone complex through the lower Danian (Fig. 7). The lithological sequence is comparable to Mull-1, with claystone below and above the sandstone complex (Adatte et al., this volume). A major difference is the occurrence of a yellow clay layer containing weathered impact glass (cheto smectite) in the claystone between 45 and 63 cm below the sandstone complex.

PGE concentrations remain at background values in the claystone below the sandstone complex, in the yellow clay layer and in the first three units of the sandstone complex (Ir $<$ 0.25 ppb; Rh $<$ 0.2 ppb; Ru $<$ 0.3 ppb; and Pd $<$ 1 ppb; Fig. 7). The top unit of the sandstone complex records a peak in Pd (#15, 1.5 ppb) a peak in Ir (0.4 ppb) and Ru (0.9 ppb). In the overlying claystones several levels record single peak values in most PGEs. The calcareous claystone (1.72 m) records peaks in Ir (0.7 ppb), Pd (1.3 ppb), and Ru (0.8 ppb). The overlying calcareous mudstone shows high Ir and Ru of 0.6 ppb and 0.8 ppb, respectively. The burrowed claystone below the KT boundary marks a third level with peak values in Ir (0.7 ppb), Rh (0.25 ppb), and Ru (1.1 ppb), whereas Pd concentrations remain constant at 1.3 ppb and decrease at the KT boundary. In the lower Danian, Ir and Rh return to constant background values, whereas Ru records two single peaks at 0.7 ppb and a single Pd peak at 3.3 ppb.

Darting Minnow Creek DMC-1 Section

The DMC-1 section spans across the Darting Minnow Creek waterfall (Fig. 2) and encompasses the uppermost Maastrichtian including the sandstone complex of the waterfall and the lower Danian

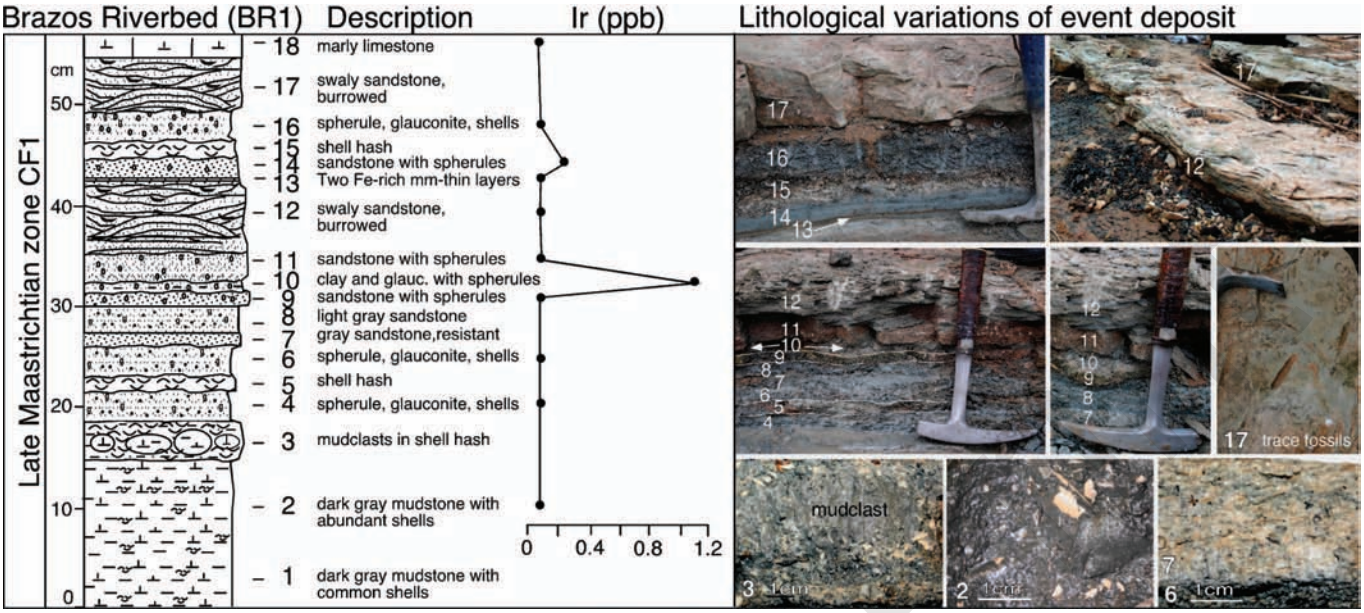

FIGURE 4.—Lithological description and Ir record across the late Maastrichtian sandstone complex at Brazos Riverbed 1 (BR1) keyed with outcrop and thin-section pictures (numbers are indicative of the sample number). Ir shows a major peak at 1.2 ppb in thin clay layer with glauconite and spherules.

(Keller et al., this volume). Above the sandstone complex the lower Danian is mainly covered in the creek bed. Planktic foraminiferal biozones P0 and P1a(1) appear to be missing, suggesting a significant hiatus (Fig. 8).

PGE analyses are restricted to five samples collected within the sandstone complex (Fig. 8). Both Ir and Rh concentrations are within background values (< 0.1 ppb), with Ru showing similar trends, but with relatively higher values (0.4–0.5 ppb). Pd and Pt concentrations are variable, with relatively high concentrations at the base (1.05 and 1.4 ppb) and top (1.5 and 1.8 ppb) respectively, low Pd values in between, but high Pt (2.1 ppb in sample 3) at the base of a laminated sandstone layer.

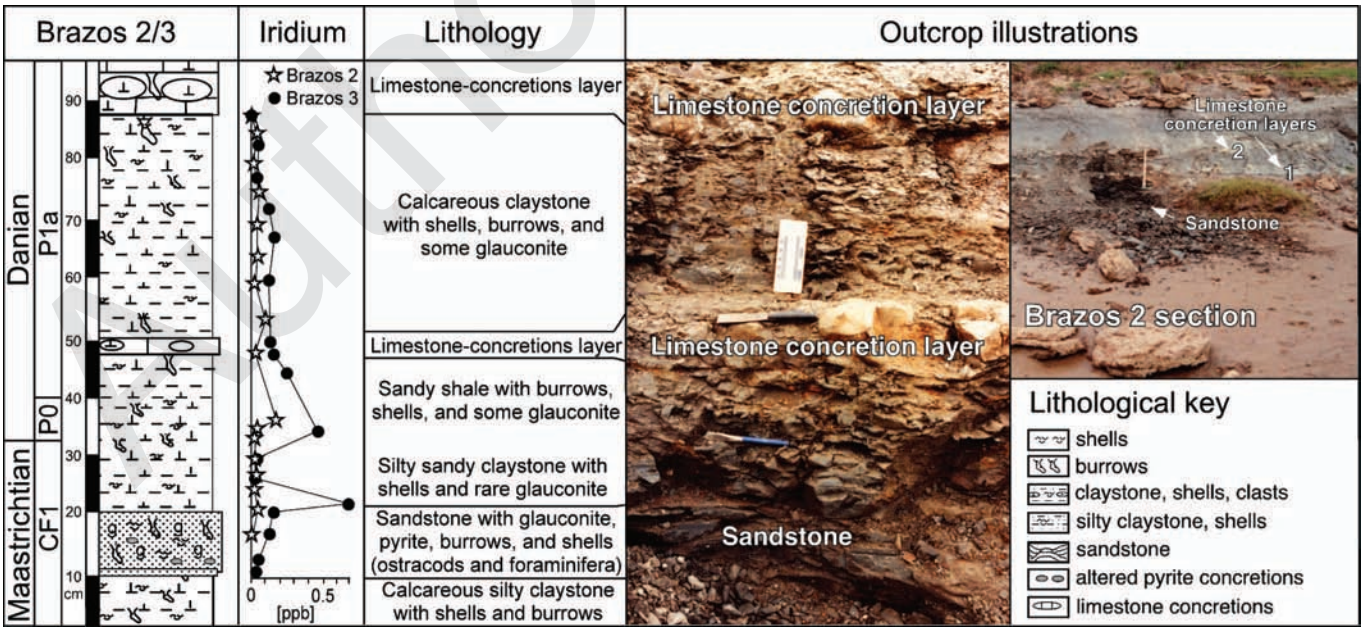

FIGURE 5.—Lithological description and Ir record of the Brazos-2 and Brazos-3 sections with outcrop illustrations. Ir trends are slightly different with higher concentrations and a peak value (0.7 ppb) above the sandstone complex at Brazos-3.

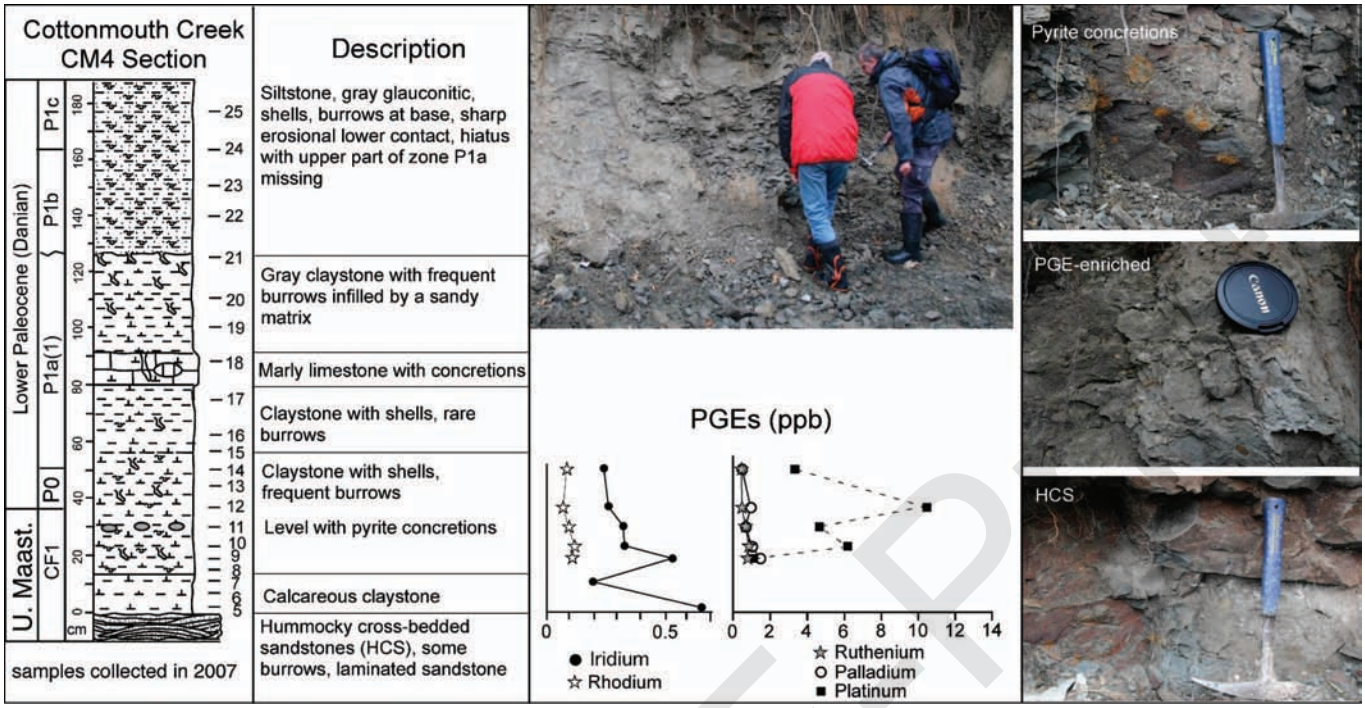

FIGURE 6.—Lithological description and PGE records for the CM4 section keyed with outcrop pictures. PGE values are usually constant, except for Ir and Pt. Ir records a maximum (0.7 ppb) above the sandstone complex and Pt peaks at 11 ppb above the KT boundary.

DISCUSSION

Correlation of PGE Profiles

In all Brazos sections, PGEs record low background concentrations generally ranging between PGE concentrations of pelagic and anoxic sediments (Table 1; Figs. 3–8). Ru values are scattered, with several single peaks, such as in the CMAB sections (Fig. 7), but concentrations remain in the range of pelagic sediments (Table 1). Rh shows no single peak in Brazos sections, and concentrations are similar to anoxic sediments (Table 1). This is probably linked with a constant detrital influx of Rh into the shallow dysoxic environment of the Brazos area during the late Maastrichtian (Keller et al, 2007; Keller et al, 2009a). All other PGEs record several single peaks with values above average pelagic sediments.

Ir concentrations are usually at background levels (0.1–0.4 ppb) in all sections and correspond to average Ir contents in sediments (Table 1). Ir peaks are rare and vary from 0.7 ppb to 1.5 ppb. Highest concentrations are encountered at the base of the laminated silty mudstone layer, as at Mullinax-1, or laminated sandstone, which commonly mark the top of the sandstone complex. In the Cottonmouth Creek sections, where this layer is absent and the HCS forms the top of the sandstone complex, elevated Ir values are observed 20 cm above in the overlying claystone (Fig. 9). Similarly, at Brazos-1 the Ir peak is 20 cm above the sandstone complex (Fig. 10). This discrepancy in the stratigraphic position of maximum Ir concentrations is likely due to variations in the local paleo-topography and hence higher sediment accumulation in topographic lows. No significant Ir enrichment is present at the KT boundary (Figs. 3–8). Ir and Ru usually peak in the same intervals (Figs. 3, 7), but these peaks cannot be correlated between several sections (Figs. 3–8). The nearly identical trends of Ir and Ru are not surprising because of their similar behavior during weathering, with redox conditions and in the presence of organic matter (Cousins and Vermaak, 1976; Evans et al., 1993).

Despite these apparent differences in PGEs between localities, the correlation of the Cottonmouth Creek sections (Fig. 9) and the Brazos River sections (Fig. 10) is surprisingly good, as also indicated by the $\delta^{13}C$ record. The discrepancies between the two transects and sites along the Brazos River and Cottonmouth Creek and Darting Minnow Creek localities to the south can easily be explained by variation in the sandstone complex. The sandstone complex was deposited in incised valleys at depths varying from estuarine (Darting Minnow Creek DMC waterfall and Mullinax-2/3 wells) to inner neritic in the Cottonmouth Creek (CMAW) and Brazos River sections (Fig. 11).

The thickness of the sandstone complex depends on the position within the incised valley. For example, in the Darting Minnow Creek, the thickest sandstone complex (1.0–1.6 m) is present in a narrow (< 20 m) incised valley. Only about 150 m away, subaerial conditions were observed in the new wells Mullinax-2 and 3 (Keller et al., this volume; Adatte et al., this volume) (Fig. 11). At Cottonmouth Creek about 1 km to the north, the sandstone complex is most expanded in the CMAW section and thins to 10 cm toward the Brazos River (Fig. 9, 11). In this transect, the CMAW section shows minor Ir concentration about 20 cm above the sandstone complex. In Cottonmouth Creek sections, where only a remnant sandstone layer is present, the maximum Ir concentrations are immediately above it (CMB, CM3-CM4; Fig. 9). This suggests concentrated sedimentation, erosion, or nondeposition at topographic highs away from the incised valley. Alternatively, variations in PGE data may be due to low concentrations, high external precision error, or nugget effects.

In the Brazos River sections, the sandstone complex is well developed, which suggests that deposition also occurred in an incised valley. However, above the sandstone complex sediment accumulation

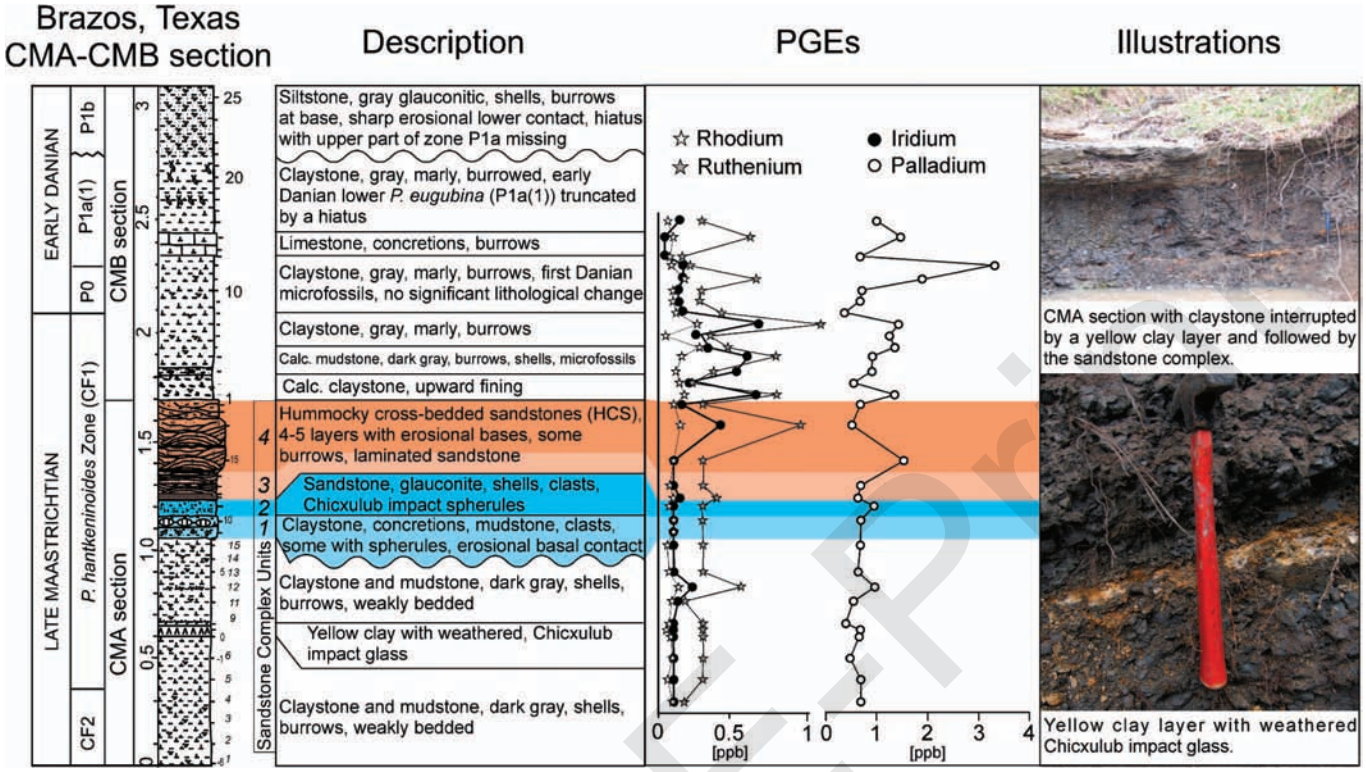

FIGURE 7.—Lithological description and PGE records for the CMA-CMB section with outcrop pictures. PGEs show scattered peaks in the upper part of the sandstone complex (unit 4) and the overlying claystone, but no PGE enrichments are recorded at the KT boundary.

was higher than in the Cottonmouth Creek transect, which indicates sedimentation in slightly deeper water and/or in a topographic low (Figs. 10, 11). Variations in the PGE stratigraphy also reflect variable topography and sediment accumulation rates. This is indicated by the maximum Ir concentration in Mullinax-1 near the top of the sandstone complex and at Brazos-1 at 20 cm above it.

Processes Responsible for PGE Patterns

Generally, PGE peaks are observed in the upper part of the sandstone complex at or close to lithological boundaries and in claystones between the sandstone complex and the KTB (Figs. 3–8). Various processes may be responsible for these scattered enrichments, including high PGE concentrations related to high organic-matter contents, link to clay minerals, influence of redox conditions, concentration by postdepositional diagenetic processes, concentration by sediment starvation, and the Chicxulub impact. PGE anomalies (especially Ir) associated with high contents of organic matter were postulated for the Triassic–Jurassic boundary (Tanner et al., 2008), but the CMAB section and the Mullinax-1 well show no correlation between total organic carbon (TOC) and PGEs (Figs. 12, 13). Clay minerals have complex compositions and often contain various trace elements, but no correlation is observed at Brazos between the major clay mineral smectite (70–100%) and PGEs (Figs. 12, 13).

Chicxulub Impact and Ir Concentrations: The major Ir peak in all Brazos sections is present in laminated silty mudstone or laminate sandstone above the hummocky cross-bedded sandstone (HCS) of the sandstone complex, which is commonly attributed to a tsunami generated by the Chicxulub impact (Ganapathy et al., 1981; Asaro et al., 1982, Bourgeois et al., 1988; Smit et al., 1996; Schulte et al., 2006). According to this model, the sedimentary sequence of the sandstone complex was deposited at the KT boundary during the span of a tsunami event. The lithological succession corresponds to a plausible sequence after an impact with deposition of clastic fractions with impact spherules, followed by finer sediments with reworked Maastrichtian fauna, Ir fallout, and settling of fines at the top. The main merit of this model is that it explains the vertical separation between the KT boundary, the Ir peaks, and impact spherules. The glass spherules are a direct marker of the Chicxulub impact, whereas Ir can originate directly from a meteorite or from an increased input of cosmic dust rich in Ir associated with the meteorite. In Brazos sections, Ir records a major peak within or above the sandstone complex (e.g., BR1, Brazos-1, Mullinax-1), followed by minor concentrations, which may be consistent with a direct meteorite input and increased input of cosmic dust.

However, this interpretation has several fundamental flaws, which lead to its rejection: (1) Chicxulub impact spherules occur at the base of the sandstone complex in two to three discrete upward-fining layers, which are reworked and do not correlate with the main Ir anomaly (Figs. 3–9) (Keller et al., 2007; Keller et al., 2008a; Keller et al., 2009a). (2) Lithified clasts with impact spherules are present at the unconformity at the base of the sandstone complex (Keller et al., 2007). These spherule-rich clasts reveal the presence of an older impact-spherule layer that was lithified, eroded, transported, and redeposited at the base of the sandstone complex. The Chicxulub impact must therefore be older than the sandstone complex. (3) A yellow clay layer that consists of altered impact-glass spherules (cheto smectite) is present in upper Maastrichtian claystones 45–60 cm below the sandstone complex and may represent the primary pre-KTB age

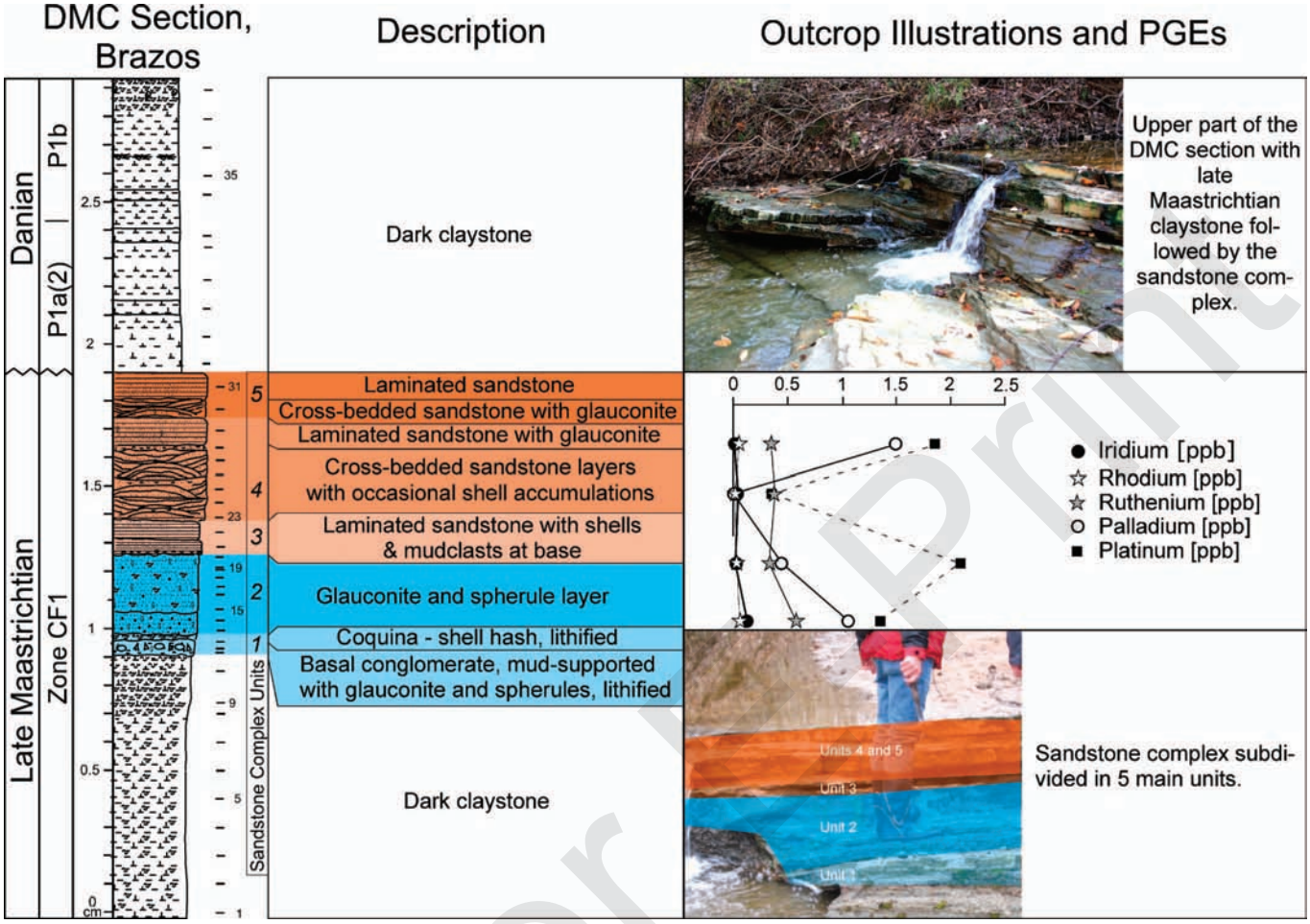

FIGURE 8.—Lithological description and PGEs of the DMC section with outcrop pictures. A major hiatus between planktic foraminifera biozones CF1 and P1a(2) occurs at the KT boundary. PGEs show usually low and constant concentrations, but Pd and Pt values are more variable, with a minimum at 1.47 m.

Chixculub impact ejecta (Keller et al., 2007; Keller et al., 2008a; Keller et al., 2009a). (4) Dark organic-rich claystones (0.8 m) separate the KT boundary from the sandstone complex and indicate the return to normal sedimentation well prior to the KT mass extinction. All of these data are inconsistent with the tsunami interpretation. They reveal a long-term scenario that includes sediment deposition during a time of climate changes, the Chicxulub impact on Yucatán, followed by a significant sea-level fall accompanied by erosion of incised valleys and subsequent infilling during the early transgression (Gale, 2006; Keller et al., 2007). In this long-term depositional scenario other sedimentary processes can explain the near absence of Ir in the sandstone complex.

PGEs and Redox Processes: All PGEs are highly sensitive to redox fluctuations, and especially the manganese cycle, but they usually show a poor correlation with Fe_{total}, Mn_{total}, redox-sensitive trace elements such as U, and other environmental proxies, such as Zn (Figs. 12, 13). However, the Mullinax-1 well shows high $Mn_{carbonate}$ concentrations in the upper part of the sandstone complex associated with several PGE peaks and generally higher PGE concentrations. Therefore higher Mn concentration in the carbonate fraction appears to promote PGE enrichments, but further detailed studies are required to confirm these observations.

Postdepositional concentrations due to redox fluctuations and/or mobility is likely for several Pd and Pt peaks due to their high sensitivity, but this remains to be confirmed (Figs. 3, 7; Cousins and Vermaak, 1976; Westland, 1981). For Ir, most peaks occur at or close to lithological boundaries, where redox conditions may fluctuate and lead to postdepositional concentration (Colodner, 1991). However, mobility of PGEs is variable for each element, and redox variations would result mainly in separating peaks of each PGE without changing the original concentrations significantly. This could be one factor responsible for the relatively poor correlation between the different PGE enrichments in the Brazos area (Figs. 9, 10).

Ir, Sea-Level, and Sediment Accumulation Rates: In Brazos sections, Ir peaks are observed in intervals between the upper part of the sandstone complex and above it, but never at the KTB. The interval with Ir enrichments was deposited in a transgressive systems tract, with the transgressive surface at the top of the sandstone complex and the maximum flooding surface at the KT boundary (Gale, 2006; Keller et al., 2007; Adatte et al., this volume). Most Brazos sections record Ir maxima at or close to the transgressive surface and smaller concentrations close to the maximum flooding surface (Figs. 9, 10). Intervals from the transgressive surface to the maximum flooding

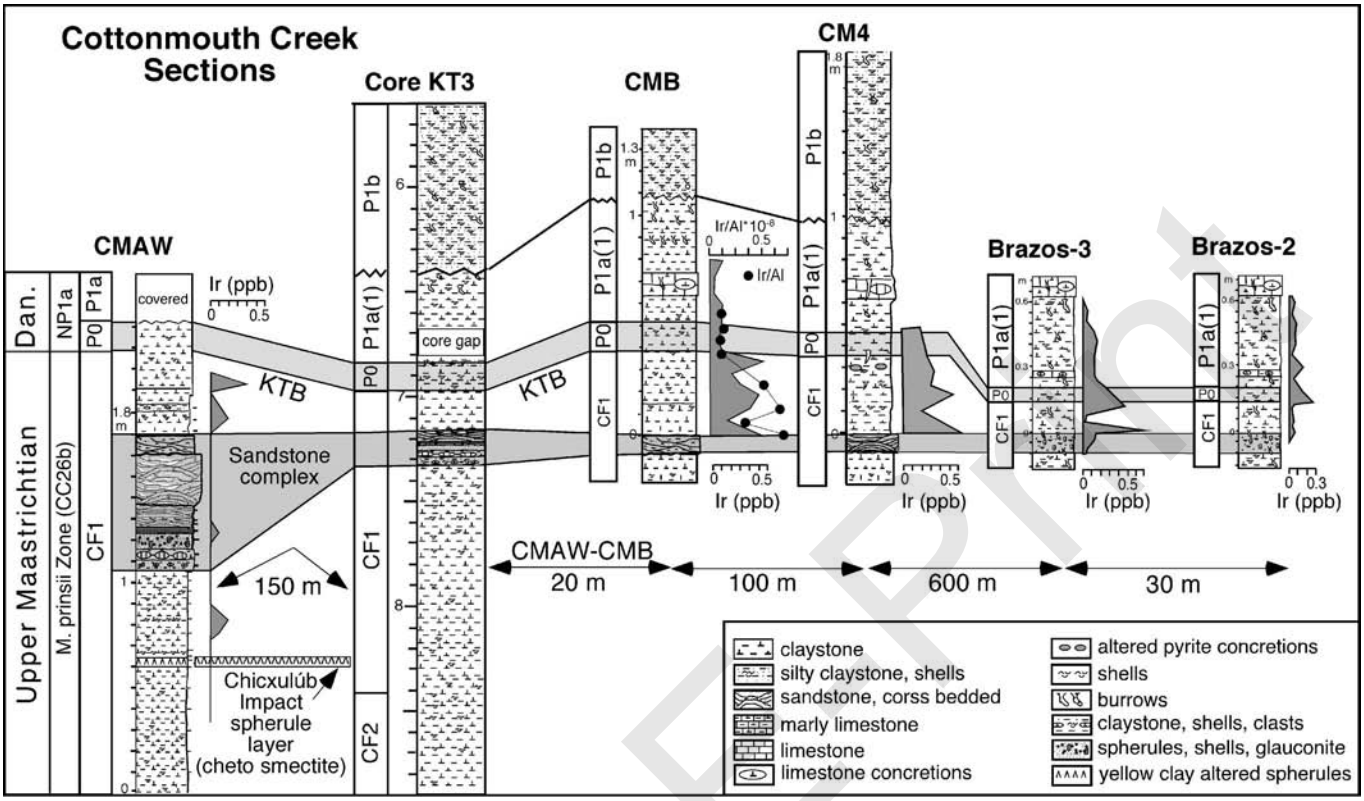

FIGURE 9.—Correlation on a west–east transect of all sections sampled along the Cottonmouth River based on lithology and Ir record. The yellow clay layer indicative of the Chicxulub impact occurs only at CMAW section. The sandstone complex is the most expanded at CMAW and thins eastward. Ir records show poor correlation but usually present a maximum above the sandstone complex.

surface are characterized by sediment starvation. Diminished or suppressed sediment supply during the terminal Maastrichtian transgressive systems tract and at the maximum flooding surface associated with the KT boundary has been postulated to explain the scattered late Maastrichtian–early Danian Ir enrichments of the nearby Braggs section, central Alabama (Donovan et al., 1988). Similarly in the Beloc sections of Haiti, Ir trends recorded from the Paleocene are related to sea-level fluctuations (Stinnesbeck et al., 1999). The scattered Ir peaks, including highs of 0.7 to 1.5 ppb in the upper Maastrichtian sandstone complex and overlying claystone at Brazos, are consistent with a sea-level fall followed by transgression accompanied by low sedimentation rates.

Absence of Ir Anomaly at KTB: Redox vs. Sedimentary Processes: The absence of an Ir anomaly at the KTB in the Brazos sections is puzzling. Could this absence be due to redox conditions and/or dilution effects? In most KTB sections worldwide, a thin (3–4 mm) red clay layer is present at the KTB and contains maximum Ir concentrations and other PGEs (Table 1). Ir concentrations in marine KTB sequences vary from $<$ 1 to 17 ppb. In general, red clay layers form in hemipelagic and pelagic regions under low sedimentation and very low rates of organic-matter accumulation (Glasby, 2006). Red clay layers at the KTB show similar characteristics (Adatte et al., 2002). In modern oceans, red clay layers have compositions similar to the average shale but are enriched in Mn, Co, Ni, and Cu (Glasby, 2006). The presence of Mn oxides in these sediments leads to scavenging of transition elements such as Co, Ni, and Cu. For example, red clays are usually enriched in Mn relative to average shale by a factor of 7, in Co by a factor of 4, in Ni by a factor of 3, in Cu by a factor of 5, and in Fe by a factor of 1.4 (Glasby, 2006). Like most PGEs, Ir is also a transition element and is strongly affected by Mn cycles (Colodner, 1991; Colodner et al., 1992). Therefore, the KTB red clay layer present in most sections provides conditions suitable for Ir enrichment and preservation.

Based on Ir data from recent marine cores, Colodner (1991, p. 153) estimated that Ir concentrations could reach up to 1.6 ppb, if the Ir lost from the halo interval during early or late diagenesis were trapped in a 1-cm-thick layer. However, it has never been shown that such conditions have been achieved in condensed sections to date. Many KTB red clay layers record Ir values above this level (Table 1) and require an extraterrestrial source. Favorable redox conditions in red clay layers are probably responsible for preservation of extraterrestrial Ir in KTB red layers but are not the main factor of enrichment. Ir can also peak at the KTB in other marine sediments, such as dark laminated clay layers (Pardo et al., 1999). In terrestrial sediments of the Raton Basin, New Mexico and Colorado, maximum Ir concentrations are observed in a kaolinitic claystone (Pillmore et al., 1984). Although this Ir peak is generally interpreted as the KTB impact event, accurate age control in terrestrial environments remains questionable and correlation to the marine KTB is based solely on the Ir anomaly.

At Brazos, the characteristic KTB red clay layer and Ir peak are absent, but planktic foraminiferal biostratigraphy (mass extinction and evolution of first Danian species) and the $\delta^{13}C$ shift mark the position of the KTB correlative to KT sections worldwide. The cause for the absence of this PGE anomaly remains to be determined. However, it is likely linked to the proximal position of the Brazos area in the Western

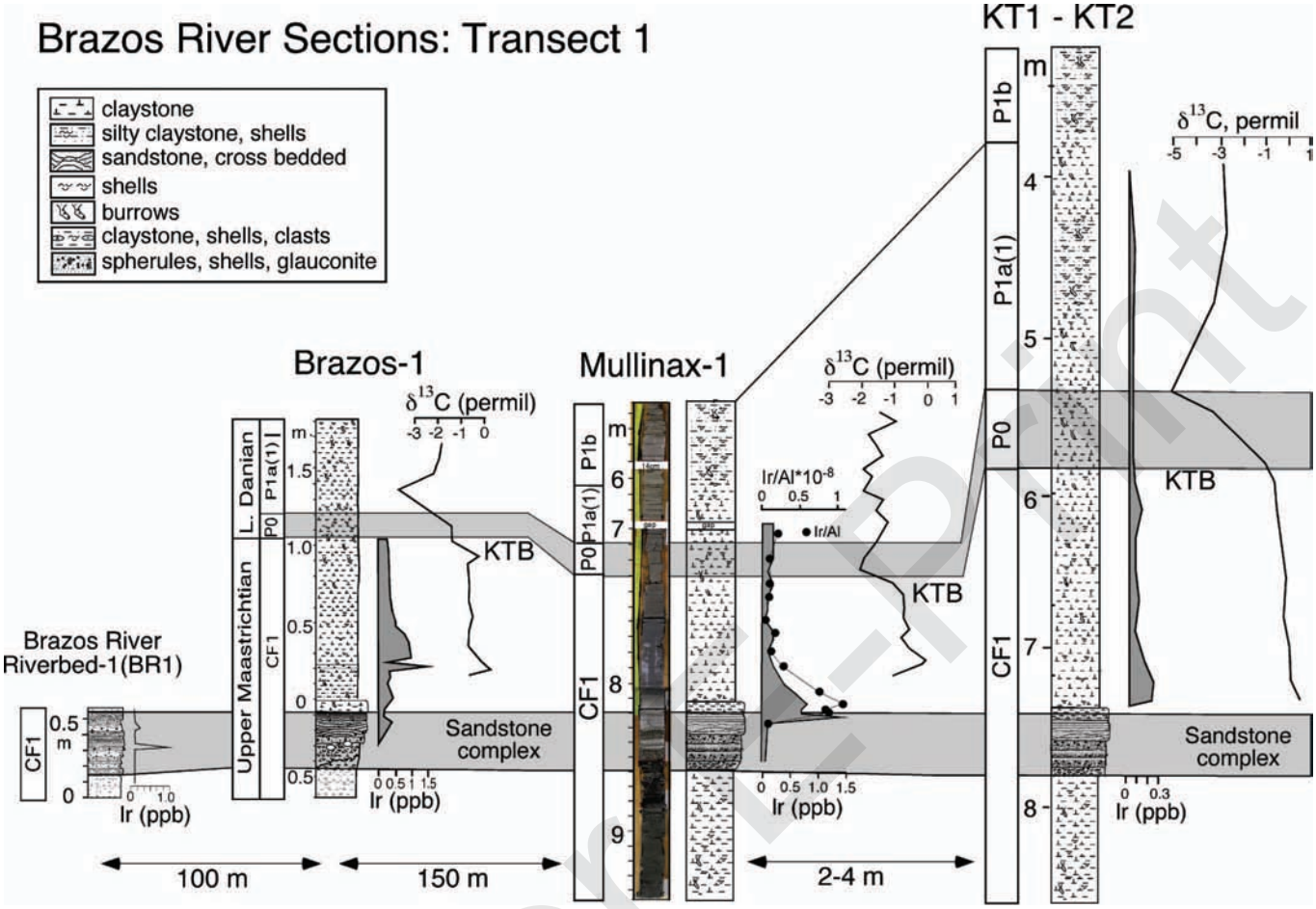

FIGURE 10.—Correlation on a west to east transect of BR-1, Brazos-1, Mullinax-1, and KT1-KT2 outcrops and cores based on lithology, carbon isotopes, and Ir. Carbon isotopes show a rapid decrease at the KT boundary above the sandstone complex. Ir trends correlate poorly but usually show higher values or peaks above the sandstone complex.

Interior Seaway and the high influx of terrestrial sediment across the KTB, which would impede the formation of a red clay layer.

Ir Enrichments and Sediment Accumulation Rates: In open marine environments, low sedimentation rates were postulated for Ir enrichment at the KTB (Kyte et al., 1985; Bruns et al., 1997). Due to the proximal location of Brazos sections, dilution effects triggered by higher sedimentation rates are likely an important factor influencing the absence of an Ir peak at the KT boundary. For example, average sedimentation rates prior to the KTB at Mullinax-1 are estimated at 2.3 cm/kyr and 0.93 cm/kyr for Mullinax-3 for planktic foraminiferal biozone CF1 (Abramovich et al., this volume). Since there is no lithological change at the KTB and no significant change in the sediment composition of the lower Danian, a very high rate of sediment accumulation likely continued across the KTB due to high terrigenous influx. In contrast, sedimentation rates in the red clay layer average 0.5 mm/kyr (Leeder, 2005; Glasby, 2006).

In order to compare Ir enrichments in different lithologies, Ir concentrations should be recalculated for similar sedimentation rates to exclude possible dilution effects. Based on simple calculations taking into account the average sedimentation rate, the thickness of the KTB layer, and the original Ir concentration, a hypothetical Ir concentration, [Ir*], can be calculated $[Ir^*] = k[Ir]S/T$, where [Ir] is the original concentration and S is the average sedimentation rate of the lithology across the KTB, assumed to be 0.5 mm/kyr for red clay layers, and T is the thickness of the KT layer, which is generally 5 mm (Table 4). K is a constant calculated based on the assumption that $[Ir] = [Ir^*]$, $S = 0.5$ mm/kyr and $T = 5$ mm in KT red clay layers. This constant is therefore equal to 10 kyr. Based on this formula, Ir concentrations of different red clay layers were recalculated and corrected for dilution effects (Table 4). Most KTB red clay layers show identical Ir enrichment, except at El Kef, where the thickness of the red clay layer is slightly lower (4 mm; Table 4).

If we apply this equation to the KT Ir concentration at Brazos (0.1 ppb) and assume a minimum sedimentation rate of 9.3 mm/kyr and a thickness of 5 mm, Ir concentration corrected for dilution effects indicates a value of 1.86 ppb (Table 4). This concentration is on the low side of most KTB [Ir*] iridium anomalies, but this calculation shows that an extraterrestrial input of Ir on Earth generated by an impact can be diluted in proximal environments, such as the Brazos area, under high sedimentation rates. Since the global Ir enrichment observed in open marine environments at the KTB indicates an increase in Ir from an extraterrestrial source, dilution or concentration under fluctuating sedimentation rates can account for only one small part of the signal.

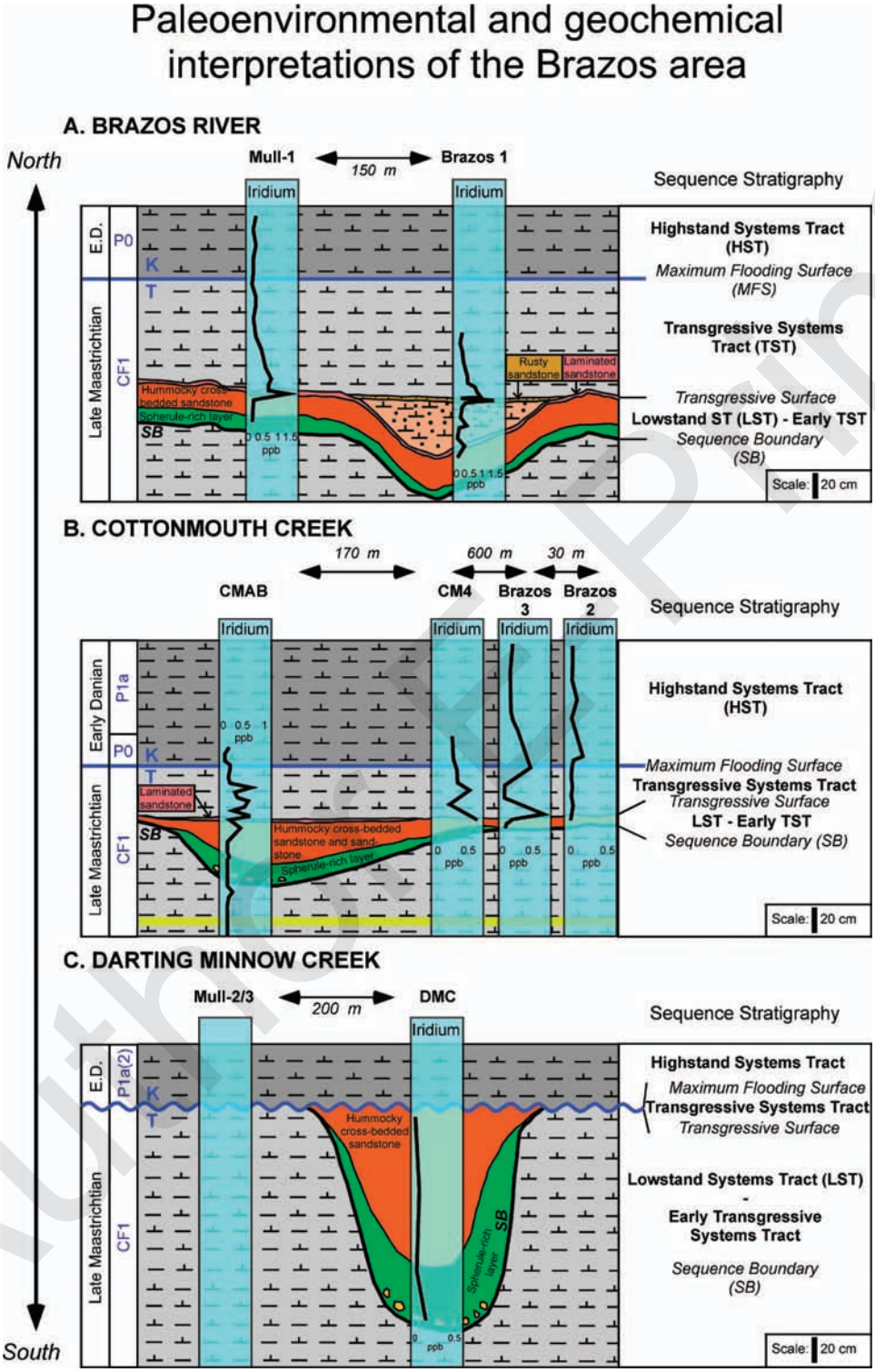

FIGURE 11.—Paleoenvironmental, geochemical, and sequence stratigraphic interpretations for three west–east transects of the Brazos area: A) for the Brazos River transect (Mull-1 core and Brazos-1 section), the main Ir anomaly occurs in a laminated sandstone at Mull-1 and in a rusty sandstone at Brazos 1 at the transgressive surface; B) in the Cottonmouth Creek transect, the major Ir anomaly occurs in a laminated sandstone at CMAB section and at the top of the hummocky cross-bedded sandstone (HCS) at CM4 and Brazos-3 sections, which correspond to the transgressive surface; C) for the Darting Minnow Creek transect, no Ir anomaly is recorded, because of the large hiatus present at the KT boundary.

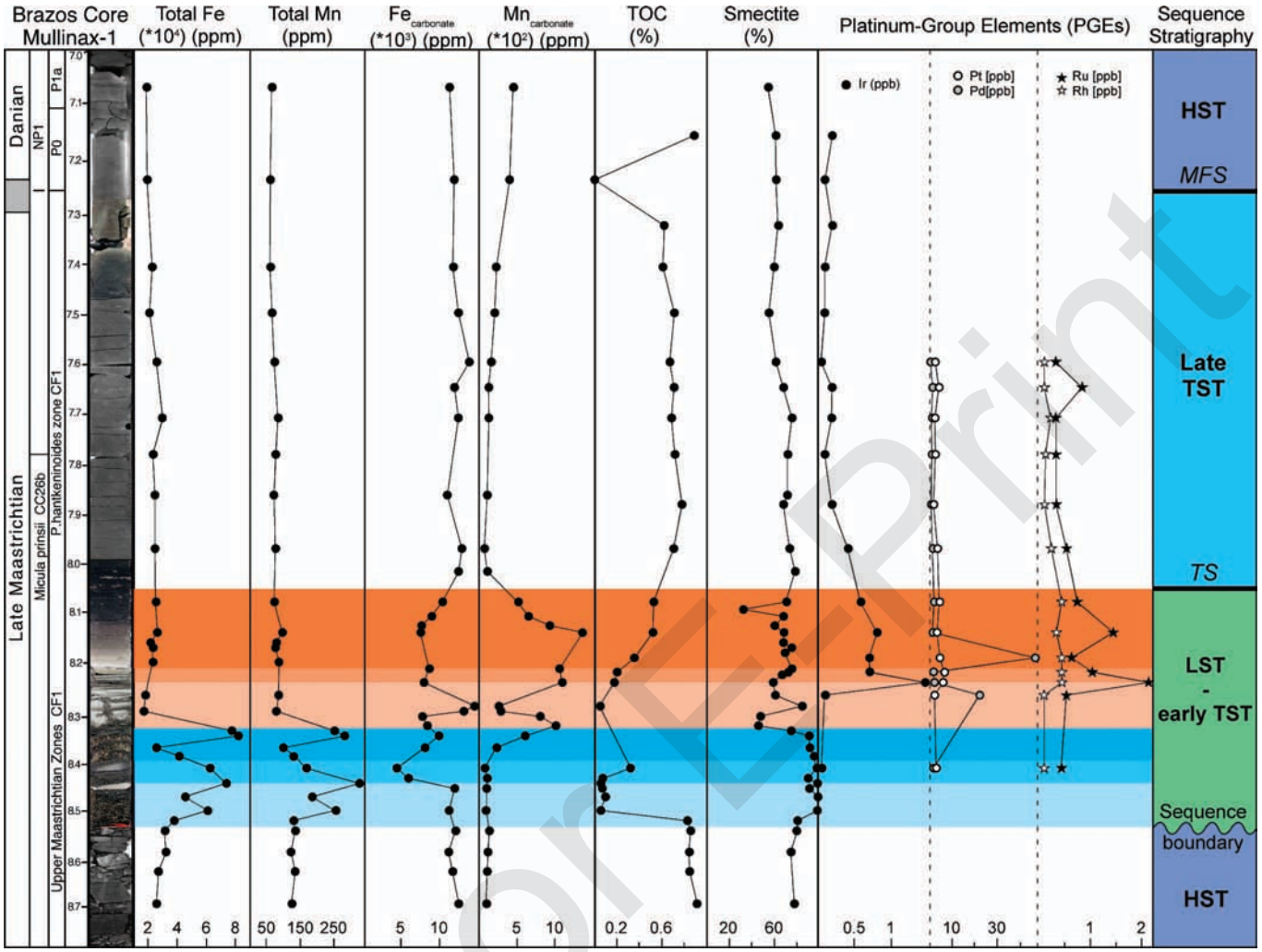

FIGURE 12.—Summary figure for Mullinax-1 core with Fe_{total}, Mn_{total}, $Fe_{carbonate}$, $Mn_{carbonate}$, total organic carbon (TOC), smectite, PGEs, and sequence stratigraphic interpretations. PGEs show a poor correlation with all proxies, but Ir records higher values where $Mn_{carbonate}$ concentrations are high. PGE peaks occur during the transgressive systems tract (TST) close to the transgressive surface (TS) when detrital supply is diminished or absent.

Therefore, other still unknown reason must explain the absence of an Ir anomaly at the KTB in the Brazos area.

We conclude that the complex Ir pattern in the Brazos sections remains enigmatic, and that further research is needed. This study and discussion explored potential factors that may explain the Ir record at Brazos and offers some preliminary conclusions: (1) No PGE enrichments correlate with the Chicxulub impact, because this impact predates the sandstone complex, where reworked spherules are encountered. (2) The minor Ir peaks present between multiple hummocky cross-bedded sandstone (HCS) and laminated sandstones are likely related to short periods of sediment starvation, but other factors, such as redox conditions, may have played a minor role. (3) The major Ir peak is correlative between all Brazos sections once variable depositional rates and local topography are considered. In all sections, Ir peaks occur at or close to a major transgressive surface where Ir can be concentrated under very low sedimentation rates. (4) Absence of an Ir anomaly at the KTB is at least partly related to dilution of the original extraterrestrial signal under high sedimentation rates at Brazos.

Among all remaining uncertainties, the major question concerns the source of Ir during the late Maastrichtian at Brazos. Non-KTB Ir enrichments have been observed in Danian sediments from Haiti, central and southern Mexico, Belize, and Guatemala (Keller et al., 2003a; Keller et al., 2003b; Stueben et al., 2005). But no prior Ir enrichments have been found to date in upper Maastrichtian sediments, except in the Brazos sections (Keller et al., 2008a). This may partly be due to the lack of PGE investigations in uppermost Maastrichtian sediments. Alternatively, increasing extraterrestrial dust input on Earth or remobilized Ir from the Chicxulub impact are potential sources for the Ir observed in the upper Maastrichtian sandstone complex and in the overlying claystone at Brazos. This possibility needs to be explored in a global study of upper Maastrichtian sediments. Finally, weathering of exposed Ir-rich intrusive rocks or continental sediments followed by their transport during the sea-level transgressive phase may also be investigated.

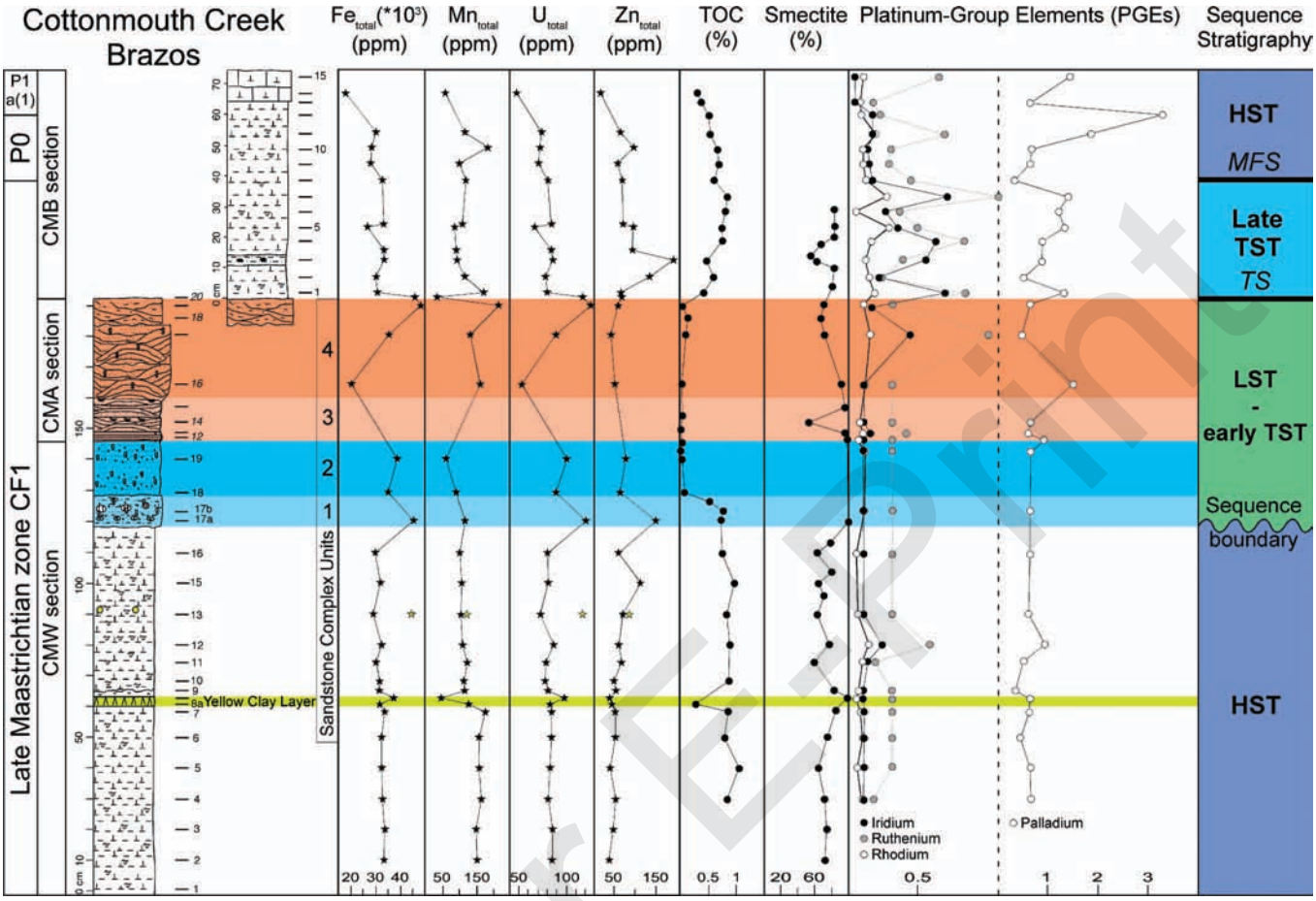

FIGURE 13.—Summary figure for CMABW section in Cottonmouth Creek with Fe_{total}, Mn_{total}, U_{total}, Zn_{total}, total organic carbon (TOC), smectite, PGEs, and sequence stratigraphic interpretations. PGEs correlate poorly with TOC, clay minerals, and redox-sensitive elements, such as Fe, Mn, U, and Zn. Most peaks are observed during the late transgressive systems tract (TST) and close to transgressive surface (TS) and maximum flooding surface (MFS), which are periods associated with sediment starvation.

Are PGEs in Brazos of Extraterrestrial, Volcanic, Sedimentary, or Redox Origin?

Although other secondary sources are possible (e.g., weathering of Ir-rich sediments or intrusive rocks), two main possible sources for PGEs in sediments were postulated: volcanic and extraterrestrial. Basaltic volcanism releases higher concentrations of PGEs, especially in Pd and Pt (Table 1), and may cause sedimentary PGE enrichments during intense volcanic activity, such as at the end of the Cretaceous (Chenet et al., 2007; Keller, et al., 2008b; Robinson et al., 2009).

TABLE 4.—Results of hypothetical Ir concentrations, [Ir*] ([Ir*]=k*[Ir]*S/T), in several red KT layers based on the average sedimentation rate (S), thickness of the KT layer (T), original Ir concentration ([Ir]) and constant k. At Brazos, high [Ir*] shows a dilution of the Ir signal at the KT boundary due to very high sedimentation rates.

(k = 10 kyr)	Ir (ppb)	K/T boundary layer thickness (mm)	Sedimentation rate (mm/kyr)	Ir* (ppb)
Meghalaya K/T boundary layer, India	12	5	0.5	12
El Kef K/T boundary layer, Tunisia	17	4	0.5	21.25
Mishor Rotem K/T boundary layer, Israel	3.2	5	0.5	3.2
Gubbio K/T boundary layer, Italy	7	5	0.5	7
Koshak K/T boundary layer, Kazakhstan	4	5	0.5	4
Stevns Klint K/T boundary, layer, Denmark	14.88	5	0.5	14.88
Brazos K/T boundary layer, Texas, USA	0.1	5	9.3	1.86

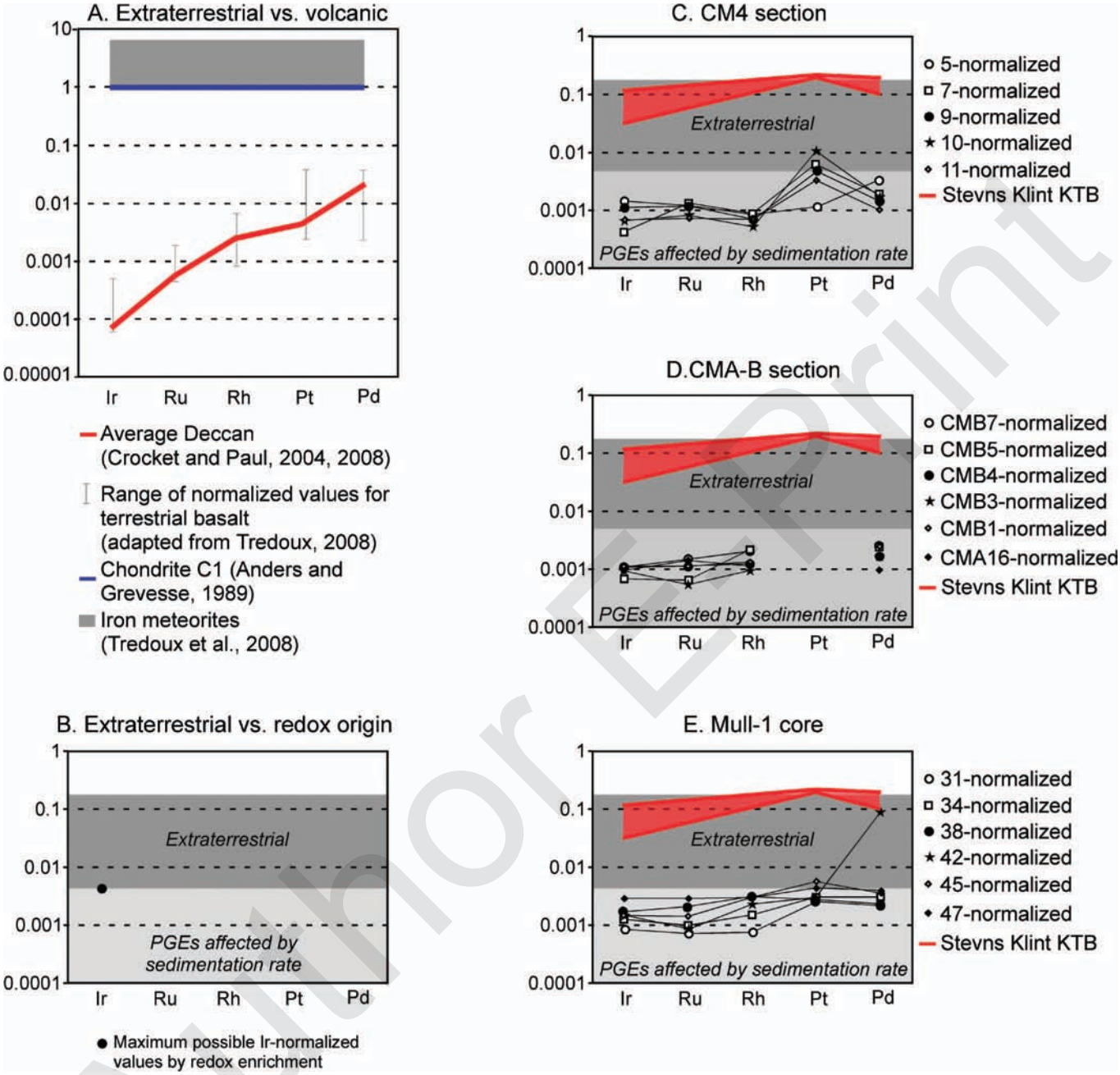

FIGURE 14.—A) PGEs normalized with chondrite for terrestrial basalt, Deccan traps, and other iron meteorites. Normalized PGEs from basalts show an oblique curve with the lowest values for Ir. B) Proposed fields to define the origin of PGEs in sedimentary rocks (adapted from Kramar et al., 2001). C) Normalized PGEs for the CM4 section with very low values indicative of a redox or sedimentary origin. For comparison, normalized PGEs for the KT boundary at Stevns Klint, Denmark, show higher ratios and a flatter trend despite the different measurement methods. D) Normalized PGEs for the CMAB section with low ratios of redox or sedimentary origin. E) Normalized PGEs for Mullinax-1 core with low ratios indicative of redox or sedimentary origin.

Meteorites, such as chondrites, contain large quantities of PGEs (Table 1) and therefore are important suppliers of PGEs on Earth. However, cosmic dust provides continuous low PGE inputs to the Earth and, to a lesser extent, volcanic activity. Accumulation of PGEs in sediments depends firstly on accumulation rate and secondly on redox conditions and periods of condensed sedimentation as discussed above for Brazos.

To differentiate between extraterrestrial and volcanic origins in sedimentary PGE records, concentrations are commonly normalized with chondrite C1 (Kramar et al., 2001; Stueben et al., 2005). When

TABLE 5.—Internal ratios between each PGE are reported for C1-chondrite, Brazos samples (Mull-1 core, and DMC, CM4 and CMB sections), and KT red layers (Stevns Klint, Meghalaya and Mishor Rotem) to test the extraterrestrial origin of PGEs.

	Ir/Pd	Ir/Pt	Ir/Ru	Ir/Rh	Pd/Pt	Pd/Ru	Pd/Rh	Pt/Ru	Pt/Rh	Ru/Rh
C1 Chondrite	**0.9**	**0.5**	**0.7**	**3.59**	**0.57**	**0.79**	**4.18**	**1.39**	**7.39**	**5.31**
Mull-1 31	0.33	0.16	0.80	4.00	0.48	2.40	12.00	5.00	25.00	5.00
Mull-1 34	0.35	0.21	0.86	3.00	0.59	2.43	8.50	4.14	14.50	3.50
Mull-1 38	0.67	0.32	0.57	2.00	0.48	0.86	3.00	1.79	6.25	3.50
Mull-1 42	0.01	0.23	1.17	2.33	16.20	81.00	162	5.00	10.00	2.00
Mull-1 45	0.37	0.13	0.70	1.75	0.35	1.90	4.75	5.50	13.75	2.50
Mull-1 47	0.64	0.33	0.67	3.50	0.51	1.05	5.50	2.05	10.75	5.25
DMC 1	0.01	0.00	0.06	0.40	0.16	4.26	29.80	27.14	190.00	7.00
DMC 2	n/d	0.01	0.07	1.00	n/d	n/d	n/d	5.71	78.00	13.67
DMC 3	n/d	n/d	n/d	n/d	0.05	1.32	22.50	25.79	438.50	17.00
DMC 5	0.11	0.09	0.21	1.71	0.79	1.83	15.14	2.33	19.29	8.29
CM4 5	0.39	0.62	0.81	6.27	1.61	2.11	16.27	1.31	10.09	7.73
CM4 7	0.19	0.03	0.22	1.67	0.17	1.14	8.75	6.60	50.58	7.67
CM4 9	0.66	0.11	0.68	5.78	0.17	1.03	8.78	6.08	52.00	8.56
CM4 10	0.35	0.03	0.55	4.57	0.09	1.59	13.14	17.84	147.86	8.29
CM4 11	0.57	0.10	0.60	3.56	0.18	1.06	6.22	6.04	35.56	5.89
CMB 7	0.38	n/d	0.50	2.00	n/d	1.32	5.33	n/d	n/d	4.04
CMB 5	0.24	n/d	0.70	1.14	n/d	4.72	4.72	n/d	n/d	1.62
CMB 4	0.55	n/d	0.65	3.19	n/d	1.18	5.81	n/d	n/d	4.94
CMB 3	0.48	n/d	1.13	3.67	n/d	2.33	7.58	n/d	n/d	3.25
CMB 1	0.40	n/d	0.68	3.00	n/d	1.70	7.56	n/d	n/d	4.44
CMA 16	0.81	n/d	0.44	3.00	n/d	0.54	3.71	n/d	n/d	6.86
KTB Stevns Klint	0.51	0.26	n/d	n/d	0.50	n/d	n/d	n/d	n/d	n/d
KTB Meghalaya	0.16	0.14	0.11	0.13	0.85	0.68	0.79	10.75	0.93	1.16
KTB Mishor Rotem	0.80	1.45	2.13	12.31	1.82	2.67	15.38	1.47	8.46	5.77

PGE compositions of different types of meteorites are normalized with chondrite C1, the resulting curves are flat with normalized values ranging from 1 to 10 (Fig. 14A). The normalization of continental basalt (e.g., Deccan basalt) shows an oblique line with increasing normalized PGE concentrations following this order: Ir $<$ Ru $<$ Rh $<$ Pt $<$ Pd (Fig. 14A). Therefore, normalized PGEs in sediments should show very different trends depending on their origin.

Normalized PGE values of the KTB red clay layers commonly show a flat line indicative of extraterrestrial origin (Kramar et al., 2001; Stueben et al., 2005). According to Kramar et al. (2001), sedimentary normalized PGE concentrations with an extraterrestrial source (impact generated) should fall within a specific area ($0.001 \leq$ normalized PGE ≤ 0.15) defined by comparing PGE compositions of several KTB red clay layers. This field is likely not accurate, because it does not differentiate impact-generated PGEs from redox-influenced PGEs, concentrated PGEs under low sedimentation rates, and diluted PGE concentrations under high sedimentation rates.

Based on the previous discussion, each element would behave differently because of the different sensitivities of PGEs to redox variations, which would therefore alter the primary impact signature for normalized values. We estimate that low sedimentation rates and sediment starvation may concentrate Ir in peaks up to 1.5 ppb at Brazos without affecting the impact signal when PGE values are normalized to C1 chondrite. Conversely, high sedimentation rates can dilute an Ir concentration of a red clay layer to background values of 0.1 ppb in claystones.

Consequently, we suggest that a new specified field should be considered that takes into account PGE concentrations influenced by sedimentation rates. Because Ir has mainly an extraterrestrial origin and can be concentrated under low sedimentation rates, and possibly redox conditions, up to average concentrations of 1.5 ppb, this element was used to define two fields: a lower field for PGEs affected by sedimentation rates (normalized PGE ≤ 0.003), and an upper field for extraterrestrial PGEs signature ($0.003 \leq$ normalized PGE; Fig. 14B).

Based on this method, most normalized PGE values for different Brazos sections (Fig. 14C, D, E) fall into the field of "Ir affected by sedimentation rates". Most samples record uneven normalized curves that may indicate a local redox influence (Figs. 14C, E). At Mullinax-1 and CMAB, some samples show very flat lines, which cannot account for an impact source because of their low PGE ratios (Fig. 14D, E). In comparison, PGE normalized data from a KTB red clay layer at Stevns Klint, Denmark, record higher values indicative of an extraterrestrial origin despite the variability in PGE measurements. Consequently, this method is a first attempt to separate primary inputs from impact or volcanism, from secondary effects, such as sedimentation rates and redox conditions. At Brazos, most results indicate that PGEs are not of impact origin but have been affected mainly by sedimentation rates and possibly by redox conditions as previously discussed.

Alternatively, let's assume that the internal PGE ratios within a sample, such as Ir/Pt or Ir/Rh, are similar to those observed in C1 chondrite, which would mean that the original impact signal is preserved in a sample. If these PGE ratios are different, PGEs could have originated from a non-extraterrestrial source or undergone secondary processes, such as diagenesis, redox fluctuations, or other unknown processes. To test this idea, we calculated internal PGE ratios for all samples of worldwide KTB red clay layers and also at Brazos (Table 5). As expected, all Brazos samples show PGE ratios very different from the C1 chondrite, which suggests the following possibilities: PGEs may be of cosmic origin or concentrated under

low sedimentation rates, or they may be affected to a minor extent by redox processes and could possibly originate from a period of increasing influx of extraterrestrial dust. Surprisingly, all KTB samples for which PGEs are available show PGE ratios very different from those calculated for the C1 chondrite (Table 5), which renders this method very doubtful, because it suggests that there was no input of extraterrestrial PGEs at the KTB. One possible explanation for these puzzling results is that the external precision of the PGE analyses and hence the reproducibility of Ir is low and that therefore values close to the chondritic ratio should be considered extraterrestrial signals.

We conclude that the proposed PGE normalizations to C1 chondrite with two separated fields (Fig. 14B) may be a good way to differentiate impact-generated PGEs from other sources and from concentrated PGEs under various processes. Further investigations on the PGE geochemistry, their normalized ratios, internal ratios within a sample, and PGE inputs from cosmic dust are required in order to define their original source in the Brazos River sections and elsewhere.

CONCLUSIONS

- Platinum group element (PGE) geochemistry of the upper Maastrichtian–lower Danian sections in the Brazos area shows complex trends that can be separated into three intervals from the late Maastrichtian to the KTB: (1) Minor peaks between units of hummocky cross-bed sandstone (HCS) of the sandstone complex; (2) major peak in laminated claystone and laminated sandstone in the uppermost part of the sandstone complex or immediately above it, depending on the local topography; (3) no PGE enrichments recorded at the KTB.
- At Brazos, PGEs, particularly Ir enrichments, always predate the KTB and coincide with a period of transgression associated with a sea-level rise (late TST and MFS), which is marked by several bioturbated surfaces and levels of reduced sedimentation that may concentrate PGEs. In several Brazos sections, the major Ir enrichment occurs at or close to a transgressive surface at or near the top of the sandstone complex. No PGE enrichments, including Ir, are recorded at the KTB. Dilution effects caused by very high sedimentation rates across the KT transition may largely account for this absence, as also suggested by the absence of a red clay layer.
- All PGE peaks in the Brazos sections show low concentrations and poor impact signatures. They appear to be mainly the result of concentration by condensed sedimentation, rather than a significant influx from a meteorite impact, though their original source remains undetermined.

ACKNOWLEDGMENTS

We gratefully acknowledge Bernd Lehman, Yuri Gavrilov, Andrei Grachev, and Art Donovan for insightful comments and suggestions. A special thank you to the owners of the Brazos Rose Ranch, Mr. and Mrs. Ronnie and Jackie Mullinax, for their permission to drill on their land and conduct fieldwork and for their gracious hospitality during our many visits. We are grateful to Jerry Baum for supervising the drilling and sharing his considerable expertise and to Tom Yancey for sharing his intimate knowledge of Brazos outcrops, for splitting the cores and description of lithology. Thanks to C. Haug and D. Munsel for fire assay analysis and C. Mössner for HR-ICP-MS measurements. The material of this study is based upon work supported by the US National Science Foundation through the Continental Dynamics Program and Sedimentary Geology Program under NSF Grants EAR-0207407 and EAR-0447171. Analytical work was supported by the Deutsche Forschungsgemeinschaft Grant Stu. 169/34.

REFERENCES

Adatte, T., Keller, G., and Stinnesbeck, W., 2002, Late Cretaceous to early Paleocene climate and sea-level fluctuations: the Tunisian record: Palaeogeography, Palaeoclimatology, Palaeoecology, v. 178, p. 165–196.

Adatte, T., Keller, G., Stueben, D., Harting, M., Kramar, U., Stinnesbeck, W., Abramovich, S., and Benjamini, C., 2005, Late Maastrichtian and K/T paleoenvironment of the eastern Tethys (Israel): mineralogy, trace and platinum group elements, biostratigraphy and faunal turnovers: Société Géologique de France, Bulletin, v. 176, p. 37–55.

Alegret, L., Arenillas, I., Arz, J.A. Díaz, C., Grajales, M., Meléndez, A., Molina, E., Rojas, R., and Soria, A., 2005, Cretaceous/Paleogene boundary deposits at Loma Capiro, central Cuba: Evidence for the Chicxulub impact: Geology, v. 33, p. 721–724.

Alvarez, L.W., Alvarez, W., Asaro, F., and Michel, H.V., 1980, Extraterrestrial cause for the Cretaceous–Tertiary boundary: Science, v. 208, p. 1095–1108.

Amosse, J., and Alibert, M., 1993, Partitioning of iridium and palladium between metals and silicate melts: evidence for passivation of the metals depending on fO2: Geochimica et Cosmochimica Acta, v. 57, p. 2395–2398.

Anbar, A.D., Wasserburg, G.J., Papanastassiou, D.A., and Andersson, P.S., 1996, Iridium in natural waters: Science, v. 273, p. 1524–1528.

Anders, E., and Grevesse, N., 1989, Abundances of the elements: meteoritic and solar: Geochimica et Cosmochimica Acta, v. 53, p. 197–214.

Asaro, H., Michel, H.V., Alvarez, W., Alvarez, L.W., Maddocks, R.F., and Burch, T., 1982, Iridium and other geochemical profiles near the Cretaceous–Tertiary boundary in a Brazos River section in Texas, *in* Maddocks, R., ed., Texas Ostracoda: Eighth International Symposium On Ostracoda, Houston, Texas p. 238–241.

Barker, J., and Anders, E., 1968, Accretion rate of cosmic matter from Ir and Os in deep sediments: Geochemica et Cosmochimica Acta, v. 32, p. 627–645.

Barnes, S.-J., Naldrett, A.J., and Gorton, M.P., 1985, The origin of the fractionation of platinum-group elements in terrestrial magmas: Chemical Geology, v. 53, p. 303–323.

Bekov, G.I., Letokhov, V.S., Radaev, V.N., Baturin, G.N., Egorov, A.S., Kursky, A.N., and Narseyev, V.A., 1984, Ruthenium in the ocean: Nature, v. 312, p. 748–750.

Bertine, K.K., Koide, M., and Goldberg, E.D., 1993, Apects of rhodium chemistry: Marine Chemistry, v. 42, p. 199–210.

Bertine, K.K., Koide, M., and Goldberg, E.D., 1996, Comparative marine chemistries of some trivalent metals-bismuth, rhodium and rare earth elements: Marine Chemistry, v. 53, p. 89–100.

Bhandary, N., Gupta, M., Panday, J., and Shukla, P.N., 1994, Chemical profiles in K/T boundary section of Meghalya, India: cometary, asteroidal or volcanic: Chemical Geology, v. 113, p. 45–60.

Bourgeois, J., Hansen, T.A., Wiberg, P., and Kauffman, E.G., 1988, A tsunami deposit at the Cretaceous–Tertiary boundary in Texas: Science, v. 141, p. 567–570.

Bruns, P., Rakoczy, H., Pernicka, E., and Dullo, W.-C., 1997, Slow sedimentation and Ir anomaly at the Cretaceous/Tertiary boundary: Geologische Rundschau, v. 86, p. 168–177.

Campell, I.H., Naldrett, A.J., and Barnes, S.J., 1983, A model for the origin of the platinum-rich sulfide horizons in the Bushveld and Stillwater Complex: Journal of Petrology, v. 24, p. 133–165.

Chenet, A.-L., Quidelleur, X., Fluteau, F., Courtillot, V., and Bajpai, S., 2007, $^{40}K/^{40}Ar$ dating of the Main Deccan large igneous province: Further evidence of KTB age and short duration: Earth and Planetary Science Letters, v. 263, p. 1–15.

Colodner, D.C., 1991, The marine Geochemistry of Rhenium, Iridium and Platinum: Ph.D. thesis, Woods Hole Oceanographic Institution and Massachusetts Institute of Technology, 269 p.

Colodner, D.C., Boyle, E.A., Edmond, J.M., and Thomson, J., 1992, Post-depositional mobility of platinum, iridium, and rhenium in marine sediments: Nature, v. 358, p. 402–404.

Cousins, C.A., and Vermaak, C.F., 1976, The contribution of Southern African ore deposits to the geochemistry of the platinum group metals: Economic Geology, v. 71, p. 287–305.

Crocket, J.H., 2000, PGE in fresh basalt, hydrothermal alteration products, and volcanic incrustations of Kilauea volcano, Hawaii: Geochimica et Cosmochimica Acta, v. 64, p. 1791–1807.

Crocket, J.H., and Huo, H.Y., 1979, Sources for gold, palladium and iridium in deep-sea sediments: Geochimica et Cosmochimica Acta, v. 43, p. 831–842.

Crocket, J.H., and Paul, D.K., 2004, Platinum-group elements in Deccan mafic rocks: a comparison of suites differentiated by Ir contents: Chemical Geology, v. 208, p. 273–291.

Crocket, J.H., and Paul, D.K., 2008, Platinum-group elements in igneous rocks of the Kutch rift basin, NW India: Implications for relationships with the Deccan volcanic province: Chemical Geology, v. 248, p. 239–255.

Crocket, J.H., MacDougall, J.D., and Harriss, R.C., 1973, Gold, palladium and iridium in marine sediments: Geochimica et Cosmochimica Acta, v. 37, p. 2547–2556.

Donovan, A.D., Baum, G.R., Blechschmidt, G.L., Loutit, T.S., Pflum, C.E., and Vail, P.R., 1988, Sequence stratigraphic setting of the Cretaceous–Tertiary Boundary in Central Alabama, *in* Wilgus, C.K., Hastings B.K., Posamentier, H., Van Wagoner, J., Ross, C.A., and Kendall, C.G.St.C., eds., Sea-Level Changes—An integrated Approach: SEPM, Special Publication 42, p. 299–307.

Dyer, B.D., Lyalikova, N.N., Murray, D., Doyle, M., Kolesov, G.M., and Krumbein, W.E., 1989, Role of microorganisms in the formation of iridium anomalies: Geology, v. 17, p. 1036–1039.

Ekdale, A.A., and Bromley, R.G., 1984, Sedimentology and ichnology of the Cretaceous–Tertiary boundary in Denmark: Implications for the causes of the terminal Cretaceous extinction: Journal of Sedimentary Petrology, v. 54, p. 681–703.

Ekdale, A.A., and Stinnesbeck, W., 1998, Trace fossils in Cretaceous–Tertiary (KT) boundary beds in Northeastern Mexico: Implications for sedimentation during KT boundary event: Palaios, v. 13, p. 593–602.

Evans, N.J., and Chai, C.F., 1997, The distribution and geochemistry of platinum-group elements as event markers in the Phanerozoic: Palaeogeography, Palaeoclimatology, Palaeoecology, v. 132, p. 373–390.

Evans, N.J., Gregoire, D.C., Goodfellow, W.D., MacInnes, B.I., Miles, N., and Veizer, J., 1993, Ru/Ir ratios at the Cretaceous–Tertiary boundary: Implications for PGE sources and fractionation within ejecta cloud: Geochimica et Cosmochimica Acta, v. 57, p. 3149–3158.

Evans, D.M., Buchanan, D.L., and Hall, G.E.M., 1994, Dispersion of platinum, palladium and gold from the main suphide zone, Great Dyke, Zimbabwe: Institution of Mining and Metallurgy Section B, Transactions, Applied Earth Science, v. 103, p. B57-B67.

Gale, A., 2006, The Cretaceous–Tertiary boundary on the Brazos River, Falls County, Texas: evidence for impact-induced tsunami sedimentation?: Proceedings of the Geologists' Association, v. 117, p. 1–13.

Ganapathy, R., Gartner, S., and Jiang, M.J., 1981, Iridium anomaly at the Cretaceous–Tertiary boundary in Texas: Earth and Planetary Science Letters, v. 54, p. 393–396.

Gertsch, B., Keller, G., Adatte, T. and Berner, Z., in preparation, The K/T transition in Meghalaya, NE India.

Glasby, G.P., 2006, Manganese: Predominant role of nodules and crusts, *in* Schulz, H.D., and Zabel, M., eds., Marine Geochemistry: Berlin, Springer, p. 371–427.

Goldberg, E.D., 1987, Comparative chemistry of the platinum and other heavy metals in the marine environment: Pure & Applied Chemistry, v. 59, p. 565–571.

Goldberg, E.D., Hodge, V., Kay, P., Stallard, M., and Koide, M., 1986, Some comparative marine chemistries of platinum and iridium: Applied Geochemistry, v. 1, p. 227–232.

Graup, G., and Spettel, B., 1989, Mineralogy and phase-chemistry of an Ir-enriched pre-K/T layer from the Lattenbirge, Bavarian Alps, and significance for the KTB problem: Earth and Planetary Science Letters, v. 95, p. 271–290.

Hallam, A., 1987, End-Cretaceous mass extinction event: Argument for terrestrial causation: Science, v. 238, p. 1237–1242.

Hansen, T.A., Farrand, R., Montgomery, H., Bilman, H., and Blechschmidt, G., 1987, Sedimentary and extinction patterns across the Cretaceous–Tertiary boundary interval in east Texas: Cretaceous Research, v. 8, p. 229–252.

Hildebrand, A.R., Penfield, G.T., Kring, D.A., Pilkington, M., Camargo, A., Jabosen, S.B., and Boynton, W., 1991, Chicxulub Crater: a possible Cretaceous/Tertiary boundary impact crater on the Yucatan Peninsula, Mexico: Geology, v. 19, p. 867–871.

Hildebrand, A.R., Pilkington, M., Connors, M., Ortiz-Aleman, C., and Chavez, R.E., 1995, Size and structure of the Chicxulub crater by horizontal gravity gradients and cenotes: Nature, v. 376, p. 415–417.

Jehanno, C., Boclet, D., Froget, L., Lambert, B., Robin, E., Rocchia, R., and Turpin, L., 1992, The Cretaceous–Tertiary boundary at Beloc, Haiti: No evidence for an impact in the Caribbean Area: Earth and Planetary Science Letters, v. 109, p. 229–241.

Jiang, M.J., and Gartner, S., 1986, Calcareous nannofossil succession across the Cretaceous/Tertiary boundary in east-central Texas: Micropaleontology, v. 32, p. 232–255.

Kalleymeyn, G.W., Rubin, A.E., Wang, D., and Wasson, J.T., 1989, Ordinary chondrites: Bulk compositions, classifications, lithophile-element fractionations, and composition petrographic type relations: Geochimica et Cosmochimica Acta, v. 53, p. 2747–2767.

Keays, R.R., 1995, The role of komatiitic and picritic magmatism and S-saturation in the formation of ore deposits: Lithos, v. 34, p. 1–18.

Keller, G., 1989, Extended Cretaceous/Tertiary boundary extinctions and delayed population change in planktonic foraminifera from Brazos River, Texas: Paleoceanography, v. 4, p. 287–332.

Keller, G., 2008, Impact Stratigraphy: old principle—new reality: Geological Society of America Special Paper 437, p. 147–178.

Keller, G., Stinnesbeck, W., and Lopez-Oliva J.G., 1994, Age, deposition and biotic effects of the Cretaceous/Tertiary boundary event at Mimbral, NE Mexico: Palaois, v. 9, p. 144–157.

Keller, G., Li, L., and MacLeod, N., 1995, The Cretaceous/Tertiary boundary stratotype section at El Kef, Tunisia: How catastrophic was the mass extinction?: Palaeogeography, Palaeoclimatology, Palaeoecology, v. 119, p. 221–254.

Keller, G., Lopez-Oliva, J.G., Stinnesbeck, W., and Adatte, T., 1997, Age, stratigraphy, and deposition of near-K/T siliciclastic deposits in Mexico: Relation to bolide impact?: Geological Society of America, Bulletin, v. 109, p. 410–428.

Keller, G., Adatte, T., Stinnesbeck, W., Stueben, D., and Berner, Z., 2001, Age, chemo- and biostratigraphy of Haiti spherule-rich deposits: a multi-event KT scenario: Canandian Journal of Earth Sciences, v. 38, p. 197–227.

Keller, G., Adatte, T., Stinnesbeck, W., Affolter, M., Schilli, L., and Lopez-Oliva, J.G., 2002, Multiple Spherule Layers in the late Maastrichtian of northeastern Mexico, *in* Koeberl, C., and MacLeod, K.G., eds., Catastrophic events and mass extinctions: impacts and beyond: Geological Society of America, Special Paper 356, Boulder, Colorado, p. 145–162.

Keller, G., Stinnesbeck, W., Adatte, T., and Stueben, D., 2003a, Multiple impacts across the K/T boundary: Earth-Science Reviews, v. 62, p. 327–363.

Keller, G., Stinnesbeck, W., Adatte, T., Holland, B., Stueben, D., Harting, M., de Leon, C., and de Cruz, J., 2003b, Spherule deposits in Cretaceous–Tertiary boundary sediments in Belize and Guatemala: Geological Society of London, Journal, v. 160, p. 783–795.

Keller, G., Adatte, T., Stinnesbeck, W., Rebolledo-Vieyra, M., Urrutia Fuccugauchi, J., Kramar, G., and Stueben, D., 2004a, Chicxulub predates the K/T boundary mass extinction: National Academy of Sciences (USA), Proceedings, v. 101, p. 3753–3758.

Keller, G., Adatte, T., and Stinnesbeck, W., 2004b, More evidence that Chicxulub predates KT boundary: Meteoritics and Planetary Science, v. 39, p. 1127–1144.

Keller, G., Adatte, T., Berner, Z., Harting, M., Baum, G., Prauss, M., Tantawy, A., and Stueben, D., 2007, Chicxulub impact predates KT boundary: New evidence from Brazos, Texas: Earth and Planetary Science Letters, v. 255, p. 339–356.

Keller, G., Adatte, T., Baum, G., and Berner, Z., 2008a, Reply to "Chicxulub impact predates K–T boundary: New evidence from Brazos, Texas" Comment by Schulte et al.: Earth and Planetary Science Letters, v. 269, p. 621–629.

Keller, G., Adatte, T., Gardin, S., Bartolini, A., and Bajpai, S., 2008b, Main Decan volcanism phase near the K–T boundary: Evidence from the Krishna Godavari Basin, SE India: Earth and Planetary Science Letters, v. 268, p. 293–311.

Keller, G., Abramovich, S., Berner, Z., and Adatte, T., 2009a, Biotic effects of the Chicxulub impact, KT catastrophe and sea level change in Texas: Palaeogeography, Palaeoclimatology, Palaeoecology, v. 271, p. 52–68.

Keller, G., Adatte, T., Berner, Z., Pardo, A., and Lopez-Oliva, L., 2009b, New evidence concerning the age and biotic effects of the Chicxulub impact in Mexico: Geological Society of London, Journal, v. 166, p. 393–411.

Koeberl, C., 1992, Water content of glasses from the K/T boundary, Haiti: An indication of impact origin: Geochemica et Cosmochemica Acta, v. 56, p. 4329–4332.

Kramar, U., Stueben, D., Berner, Z., Stinnesbeck, W., Philipp, H., and Keller, G., 2001, Are Ir snomalies sufficient and unique indicators for cosmic events?: Planetary and Space Science, v. 49, p. 831–837.

Kring, D.A., 2007, The Chicxulub impact event and its environmental consequences at the Cretaceous–Tertiary boundary: Palaeogeography, Palaeoclimatology, Palaeoecology, v. 255, p. 4–21.

Kyte, F.T., and Wasson, J.T., 1986, Accretion rate of extraterrestrial matter: iridium deposited 33 to 67 million years ago: Science, v. 232, p. 1225–1229.

Kyte, F.T., Smit, J., and Wasson, J.T., 1985, Siderophile interelement variations in the Cretaceous–Tertiary boundary sediments from Caravaca, Spain: Earth and Planetary Science Letters, v. 73, p. 183–195.

Leeder, M., 2005, Sedimentology and Sedimentary Basins; From Turbulence to Tectonics: Blackwell Publishing, Oxford, UK, 592 p.

Lehmann, B., Nagler, T.F., Holland, H.D., Wille, M., Mao, J., Pan, J., Ma, D., and Dulski, P., 2007, Highly metalliferous carbonaceous shale and Early Cambrian seawater: Geology, v. 35, p. 403–406.

Leroux, H., Rocchia, R., Froget, L., Orue-Etxebarrian, X., Doukhan, J.-C., and Robin, E., 1995, The K/T boundary at Beloc (Haiti): Compared stratigraphic distributions of the boundary markers: Earth and Planetray Science Letters, v. 131, p. 255–268.

Li, S.R., and Gao, Z.M., 2000, Source tracing of noble metal elements in Lower Cambrian black rock series of Guizhou–Hunan provinces, China: Science in China (ser. D), v. 43, p. 1051–1061.

McCallum, M.E., Loucks, R.R., Carlson, R.R., Cooby, E., and Doerge, T.A., 1976, Platinum metals associated with hydrothermal copper ores of the New Rambler Mine, Medicine Bow Mountains, Wyoming: Economic Geology, v. 71, p. 1429–1450.

MacLeod, K.G., Whitney, D.L., Huber, B.T., and Koeberl, C., 2006. Impact and extinction in remarkably complete Cretaceous–Tertiary boundary sections from Demerara Rise, tropical western North Atlantic: Geological Society of America, Bulletin, v. 119, p. 101–115.

Norris, R.D., Huber, B.T., and Self-Trail, J., 1999, Synchroneity of the KT oceanic mass extinction and meteorite impact: Blake Nose, western North Atlantic: Geology, v. 27, p. 419–422.

Officer, C.B., Hallaw, A., Drake, C.L., and Devine, J.D., 1987, Late Cretaceous and paroxysmal Cretaceous/Tertiary extinction: Nature, v. 326, p. 143–149.

Paktunc, A.D., and Ghandi, S.S., 1989, Hydrothermal platinum, palladium, gold mineralization associated with uranium veins, Northwest Territories, Canada: Geological Society of Finland, Bulletin, v. 61, p. 50.

Pardo, A., Adatte, T., Keller, G., and Oberhansli, H., 1999, Paleoenvironmental changes across the Cretaceous–Tertiary boundary at Koshak, Kazakhstan, based on planktic foraminifera and clay mineralogy: Palaeogeography, Palaeoclimatology, Palaeoecology, v. 154, p. 247–273.

Peach, C.L., Mathez, E.A., and Keays, R.R., 1994, Experimentally determined sulfide melt–silicate melt partition coefficients for iridium and palladium: Chemical Geology, v. 117, p. 361–377.

Piestrynski, A., and Sawlowicz, Z., 1999, Exploration for Au and PGE in the Polish Zechstein copper deposits (Kupferschiefer): Journal of Geochemical Exploration, v. 66, p. 17–25.

Pillmore, C.L., Tschudy, R.H., Orth, C.J., Gilmore, J.S., and Knight, J.D., 1984, Geologic framework of nonmarine Cretaceous–Tertiary boundary sites, Raton Basin, New Mexico and Colorado: Science, v. 223, p. 1180–1183.

Playford, P.E., McLaren, D.J., Orth, C.J., Gilmore, J.S., and Goodfellow, W.D., 1984, Iridium anomaly in the Upper Devonian of the Canning Basin, Western Australia: Science, v. 226, p. 437–439.

Pope, K.O., Ocampo, A.C., and Duller, C.E., 1991, Mexican site for K/T impact crater: Nature, v. 351, p. 105.

Robinson, N., Ravizza, G., Coccioni, R., Peucker-Ehrenbrink, B., and Norris, R., 2009, A high-resolution marine $^{187}Os/^{188}Os$ record for the late Maastrichtian: Distinguishing the chemical fingerprints of Deccan volcanism and the KP impact event: Earth and Planetary Science Letters, v. 281, p. 159–168.

Rocchia, R., Boclet, D., Bonte, P., Jehanno, C., Chen, Y., Courtillot, V., Mary, C., and Wezel, F., 1990, The Cretaceous–Tertiary boundary at Gubbio revisited: Vertical extent of the Ir anomaly: Earth and Planetary Science Letters, v. 99, p. 206–219.

Rocchia, R., Robin, E., Froget, L., and Gayraud, J., 1996, Stratigraphic distribution of extraterrestrial markers at the Cretaceous–Tertiary boundary in the Gulf of Mexico area: implications for the temporal complexity of the event, *in* Ryder, G., Fastovsky, D.E., and Gartner, S., eds., The Cretaceous–Tertiary Event and Other Catastrophes in Earth History, Geological Society of America, Special Paper 307, Boulder, Colorado p. 279–286.

Rudnick, R.L., and Gao, S., 2003, Composition of the continental crust, *in* Holland, H.D., and Turekian, K.K., eds., Treatise on Geochemistry, Elsevier, Netherland, chapter 3.01.

Sawlowicz, Z., 1993, Iridium and other platinum-group elements as geochemical markers in sedimentary environments: Palaeogeography, Palaeoclimatology, Palaeoecology, v. 104, p. 253–270.

Schmitz, B., 1988, Origin of microlayering in worldwide distributed Ir-rich marine Cretaceous/Tertiary boundary clays: Geology, v. 16, p. 1068–1072.

Schulte, P., Stinnesbeck, W., Stueben, D., Kramar, U., Berner, Z., Keller, G., and Adatte, T., 2003, Fe-rich and K-rich mafic spherules from slumped and channelized Chicxulub ejecta deposits in the northern La Sierrita area, NE Mexico: International Journal of Earth Sciences, v. 92, p. 114–142.

Schulte, P., Speijer, R., Mai, H., and Kontny, A., 2006, The Cretaceous–Paleogene (K–P) boundary at Brazos, Texas: Sequence stratigraphy, depositional events and the Chicxulub impact: Sedimentary Geology, v. 184, p. 77–109.

Schulte, P., Speijer, R.P., Brinkhuis, H., Kontny A., Caleys, P., Galeotti, S., and Smit, J., 2008, Comment on the paper; 'Chicxulub impact predates K–T boundary: New evidence from Brazos, Texas' by Keller et al. (2007): Earth and Planetary Science Letters, v. 269, p. 613–619.

Smit, J., Montanari, A., Swinburne, N.H.M., Hildebrand, A.R., Margolis, S.V., Claeys, P., Lowrie, W., and Asaro, F., 1992, Tektite-bearing, deep-water clastic unit at the Cretaceous–Tertiary boundary in northeastern Mexico: Geology, v. 20, p. 99–103.

Smit, J., Roep, Th.B., Alvarez, W., Montanari, A., Claeys, P., and Grajales-Nishimura, J. M., 1996, Coarse-grained, clastic sandstone complex at the K/T boundary around the Gulf of Mexico: Deposition by tsunami waves induced by the Chicxulub impact?, *in* Ryder, G., Fatovsky, D., and Gartner, S., eds., The Cretaceous–Tertiary Event and Other Catastrophes in Earth History: Geological Society of America, Special Paper 307, p. 151–182.

Smit, J., Van Der Gaast, S., and Lustenhouwer, W., 2004, Is the transition to post-impact rock complete? Some remarks based on XRF scanning electron microprobe and thin section analyses of the Yaxcopoil-1 core: Meteoritics and Planetary Science, v. 39, p. 1113–1126.

Stinnesbeck, W., Keller, G., dela Cruz, J., de Leon, C., MacLeod, N., and Whittaker, J.E., 1997, The Cretaceous–Tertiary transition in Guatemala: limestone breccia deposits from the South Peten basin: Geologishe Runschau, v. 86, p. 686–709.

Stinnesbeck, W., Keller, G., Adatte, T., Stueben, D., Kramar, U., Berner, Z., Desremeaux, C., and Moliere, E., 1999, Beloc, Haiti, revisited: multiple events across the KT boundary in the Caribbean: Terra Nova, v. 11, p. 303–310.

Stinnesbeck, W., Schulte, P., Lindenmaier, F., Adatte, T., Affolter, M., Schilli, L., Keller, G., Stueben, D., Berner, Z., Kramar, U., Burns, S.J., and Lopez-Oliva, J.G., 2001, Late Maastrichtian age of spherule deposits in northeastern Mexico: implication for Chicxulub scenario: Canadian Journal of Earth Sciences, v. 38, p. 229–238.

Stueben, D., Kramar, U., Harting, M., Stinnesbeck, W., and Keller, G., 2005, High-resolution geochemical record of Cretaceous–Tertiary boundary sections in Mexico: New Constraints in the K/T and Chicxulub events: Geochimica et Cosmochimica Acta, v. 69, p. 2559–2579.

Tanner, L.H., Kyte, F.R., and Walker, A.E., 2008, Multiple Ir anomalies in uppermost Triassic to Jurassic-age strata of the Blomidon Formation, Fundy basin, eastern Canada: Earth and Planetary Science Letters, v. 274, p. 103–111.

Tredoux, M., de Wit, M.J., Hart, R.J., Lindsay, N.M., Verhagen, B., and Sellschop, J.P.F., 1989, Chemostratigraphy across the Cretaceous–Tertiary boundary and a critical assessment of the iridium anomaly: Journaly of Geology, v. 97, p. 585–605.

Tredoux, M., Keller, G., Adatte, T., Gertsch, B., and Berner, Z., 2008, Is the KTB Iridium anomaly a unique cosmic marker? (abstract): American Geophysical Union, Fall Meeting, San Francisco, 2008.

Wallace, M.W., Gostin, V.A., and Keays, R.R., 1990, Acraman impact ejecta and host shales: evidence for low-temperature mobilization of iridium and other platinoids: Geology v. 18, p. 132–135.

Wasson, J.T., Xinwei, O., Wang, J., and Jerde, E., 1989, Chemical classification of iron meteorites: XI. Multi-element studies of 38 new irons and the high abundance of ungrouped irons from Antarctica: Geochimica et Cosmochimica Acta, v. 53, p. 735–744.

Wedepohl, K.H., 1995, The composition of the continental crust: Geochimica et Cosmochimica Acta, v. 59, p. 1217–1232.

Westland, A.D., 1981, Inorganic chemistry of the platinum-group elements, *in* Cabri, L.J., ed., Platinum-Group Elements: Mineralogy, Geology, Recovery: Canadian Institution for Mining and Mineral, Special Volume, v. 23, p. 7–18.

Yancey, T.E., 1995, Environmental change during the K/T boundary event, Brazos River, Texas: Geological Society of America, Conference Abstract, p. A326.

Zoller, W.H., Parrington, J.R., and Phelan Kotra, J.M., 1983, Iridium enrichment in airborne particles from Kilauea Volcano: January 1983: Science, v. 222, p. 1118–1121.